
Probing physics beyond the Standard Model: Precision physics and unconventional signatures

Shankha Banerjee (IMSc, Chennai, India)

PPD theory seminars and "Talk to NExT Theorists Day"

4th July 2024



Before I start ...



I would like to take this opportunity to thank **STFC PPD** and the **NExT Institute** for making my visit memorable.

This visit has been an incredible experience for me. I got the unique opportunity of discussing a lot of physics with many experimentalists from the **CMS**, **ATLAS**, **LHCb**, **DarkSide**, **LZ**, and **MIGDAL** collaborations.

Many thanks to the department for making me feel at home, and for involving me with the **Harwell Open Week**. **Thanks for the free t-shirt!**

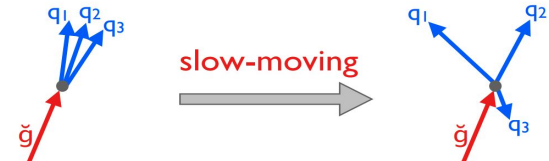
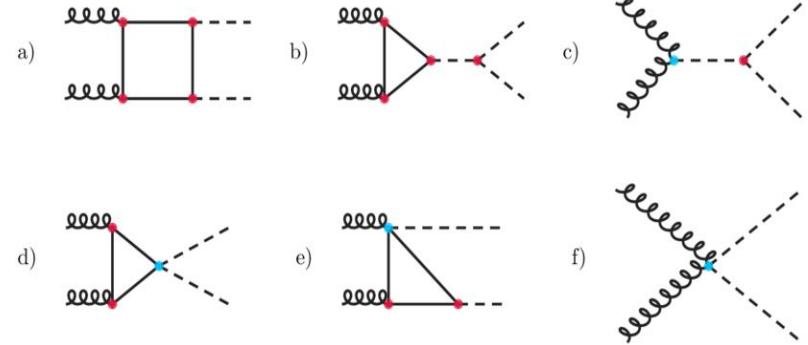
What is this talk about?

1. Why EFTs? Are they the end of the story?

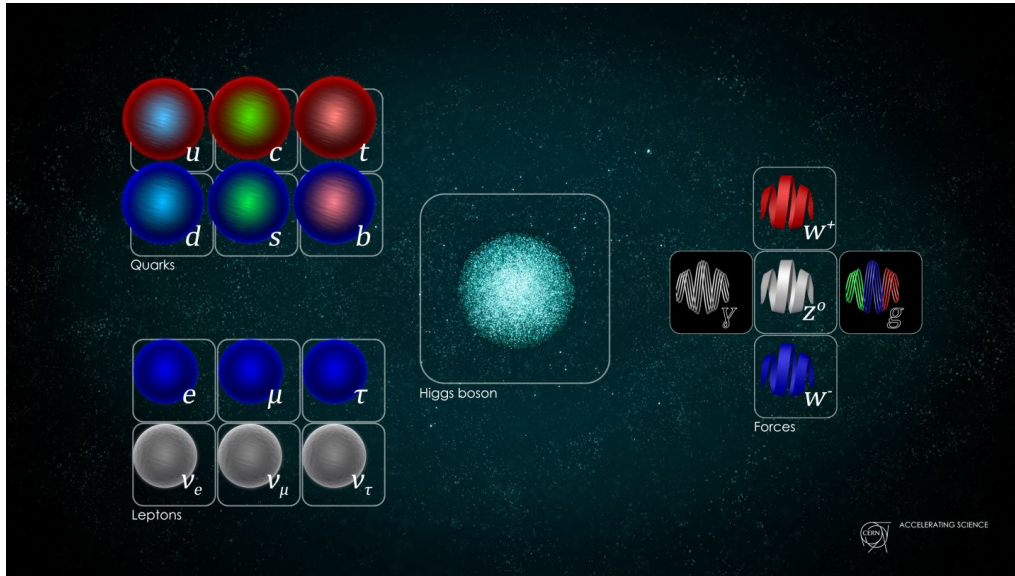
2. Why precision?

3. Why include electroweak corrections?

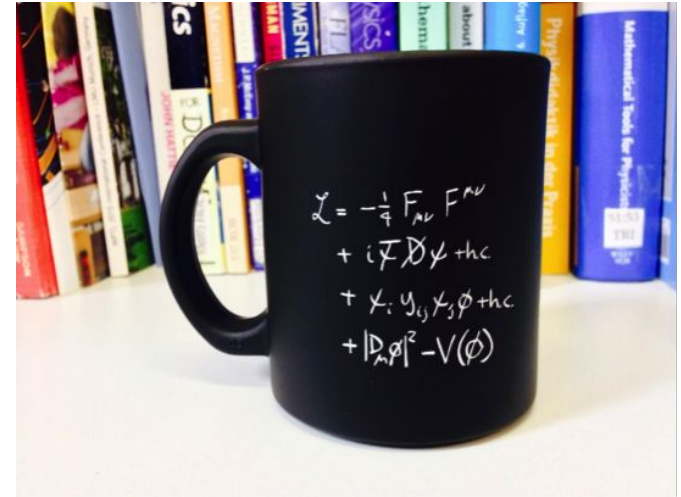
4. What do we learn from unconventional signatures?



The Standard Model of Particle Physics



Elementary particles in the Standard Model of particle physics
Image: Daniel Dominguez/CERN



Simplified way of expressing interactions between the Standard Model particles
CERN coffee mug

Why beyond the Standard Model?

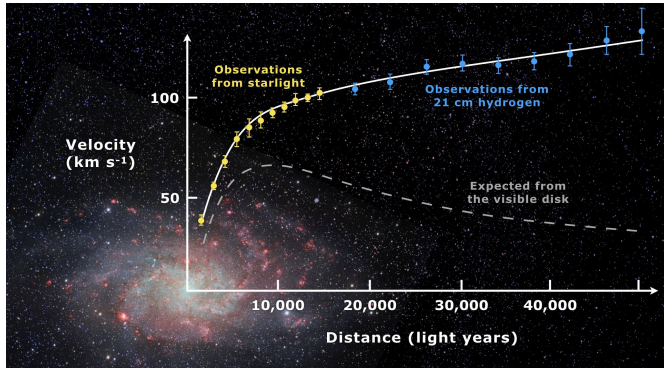


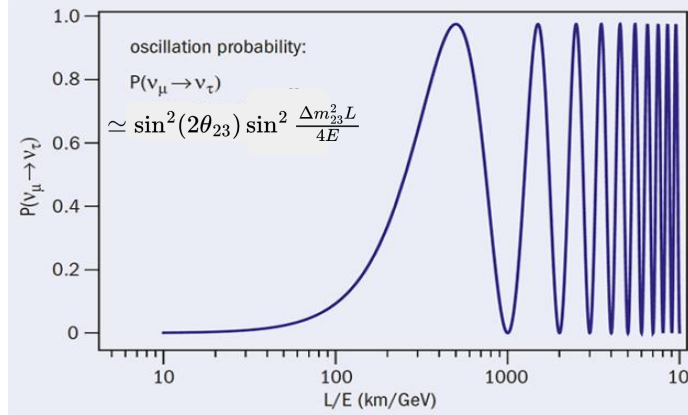
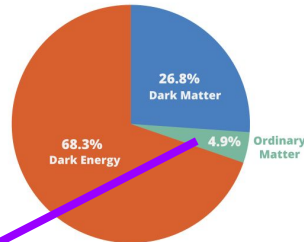
Image: Mario De Leo

Orbital speeds of visible stars/gas versus radial distance from galaxy's centre

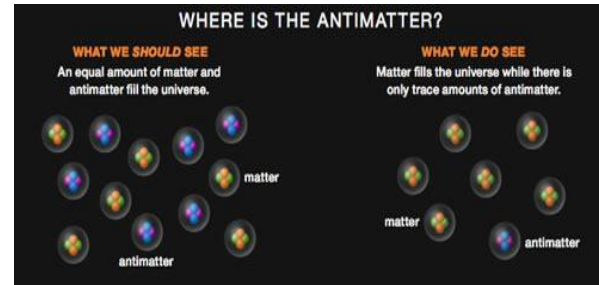
Existence of dark matter?

Whose nature we know more or less

Estimated matter-energy content of the Universe



Neutrinos change flavour while traversing distances; hence massive! What are their masses?



Baryon asymmetry!

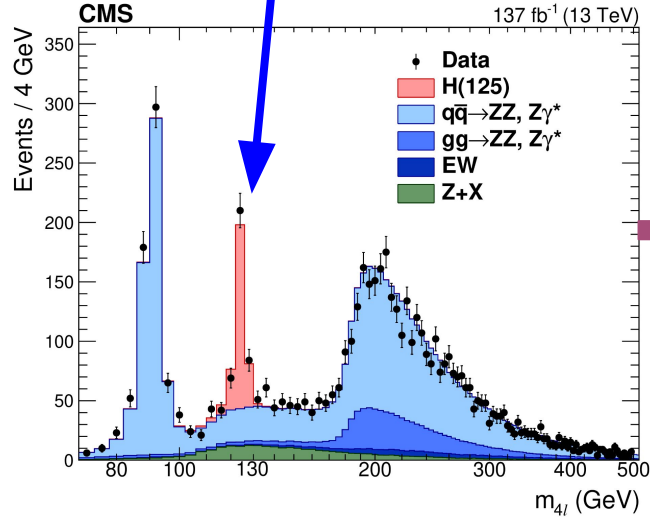
LHCb



Precision physics

Particle physics discoveries at colliders: the main types

Discovery through resonance (the tested paradigm)



We are in the phase of no BSM resonance discoveries since 2012. What to do then?

New paradigm!

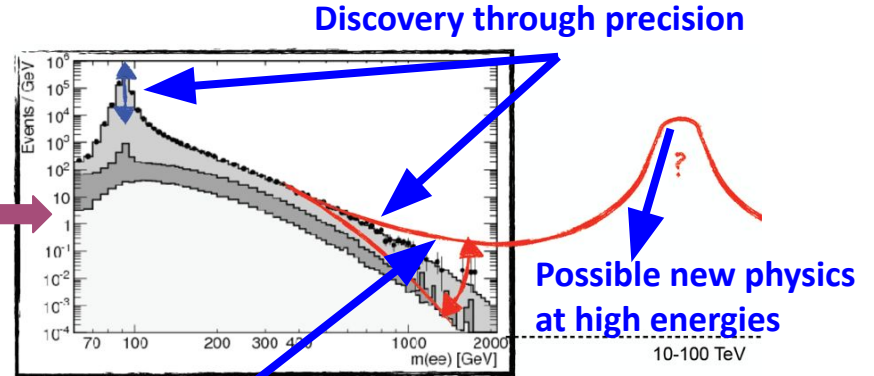
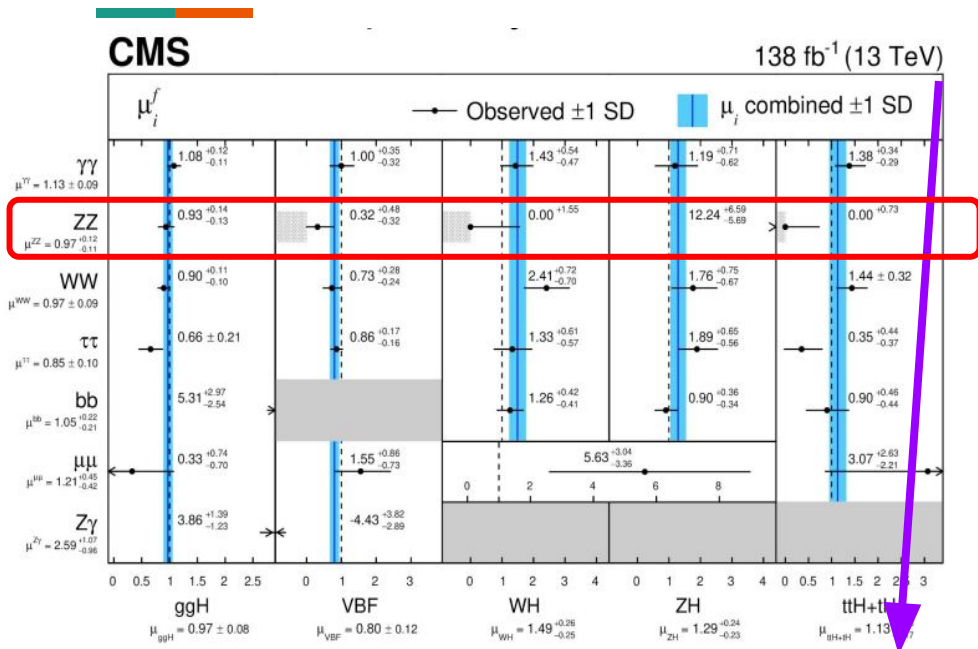


Image: Francesco Riva

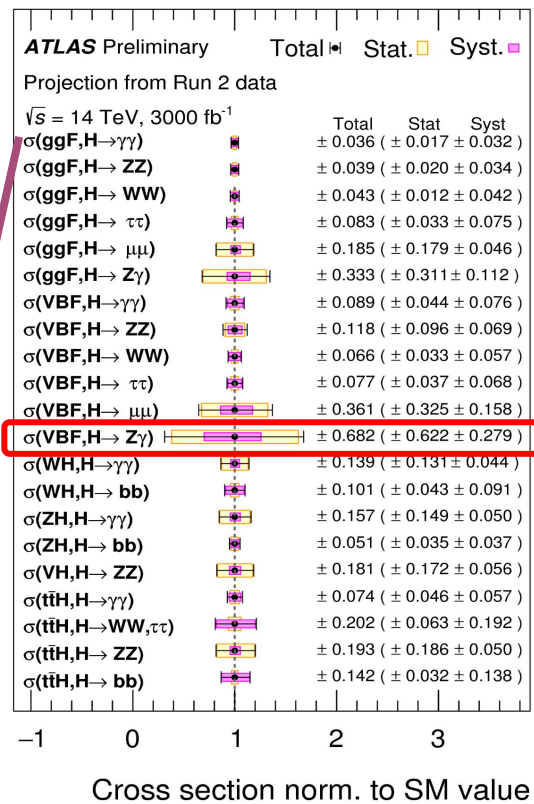
Possible to see hints of new physics through difference in heights, angular structure and tails of distributions without seeing the actual resonance.

Importance of precision: the premise



Ratios of the Higgs boson's measured interactions to other particles to its Standard Model expectations. If Standard Model predictions are exact, these numbers would eventually be 1.

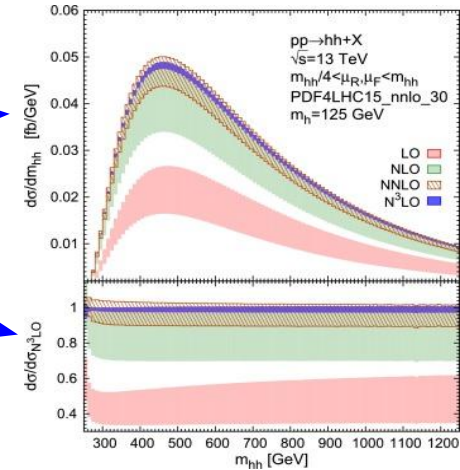
From current data



Future projections from LHC, CERN

Types of uncertainties in particle physics

- **Systematic (experimental):** instrumental uncertainties, uncertainties due to calibration of energy scales and resolution of detectors, uncertainties on detector efficiencies, etc.
- **Statistical (experimental):** stems from finite number of events recorded
- **Modelling of signal and backgrounds (theoretical):** PDF, scale, more ...
- **Luminosity:** uncertainty on precise determination of the rate of collisions
- **Monte Carlo Simulation**



Theory precision ↔ Experimental precision

Model theistic versus Model agnostic (Effective Field Theory approaches)

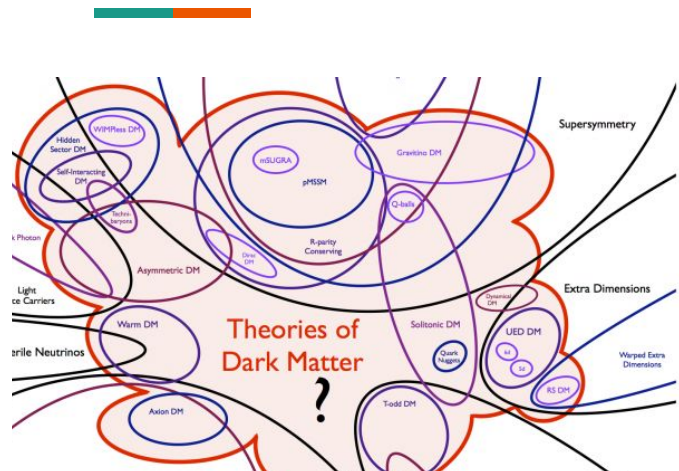


Image: Tim Tait

Imprints of new physics could show up as tiny deviations in standard measurements → Hint towards new physics?

Theory precision is thus crucial to minimise uncertainties.

No direct hints towards new physics explaining the various observations which require physics beyond the Standard Model.

No consensus. Every model comes with additional baggage which needs to be discovered.

Is new physics **hiding somewhere** that we are obviously missing?

Is the **reach just above the present experimental reach**?

Are the **interactions with Standard Model particles extremely feeble**?

Are the **theoretical and experimental precisions not good enough**?

The EFT picture

... is reinforced by the current experimental situation

$$\mathcal{L} = \mathcal{L}_{SM}^{d=4} + \sum_{d \geq 5} \sum_i \frac{c_i}{\Lambda^{d-4}} \mathcal{O}_i^d \dots$$

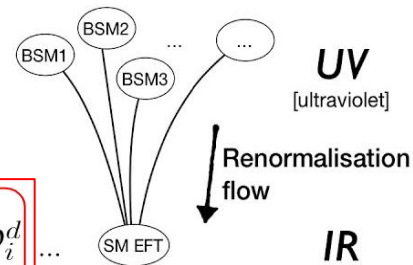
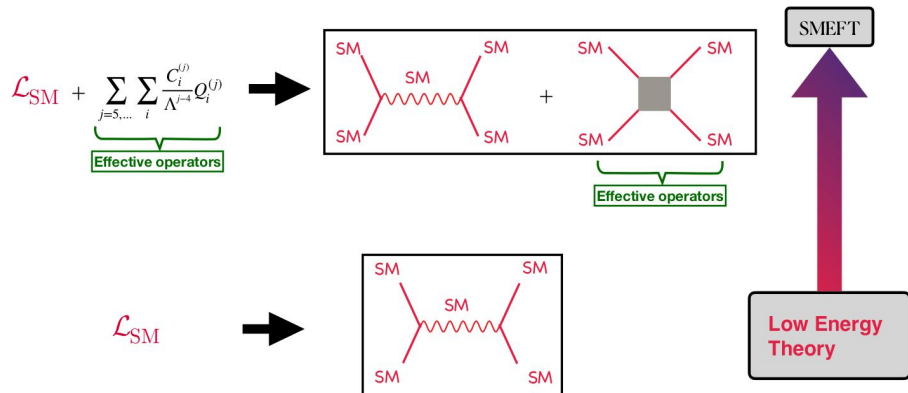


Image: Admir Greljo

Standard Model Effective Field Theory: the types

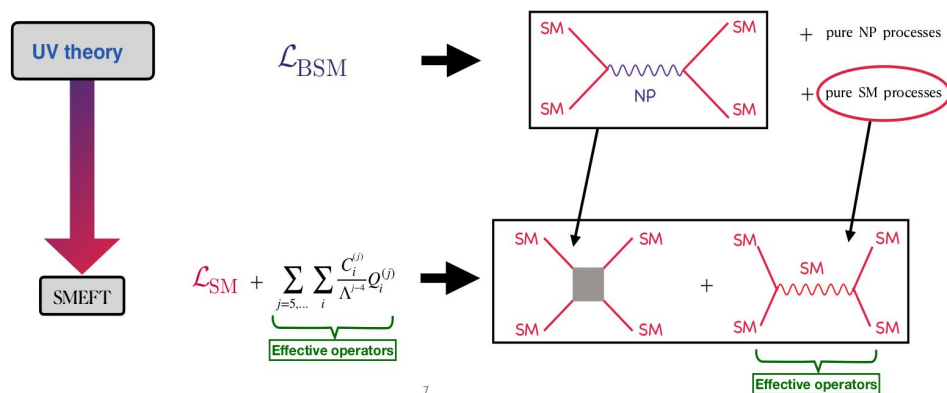
Bottom-Up approach

1. Exact nature of new physics need not be known
2. Wilson Coefficients are free parameters

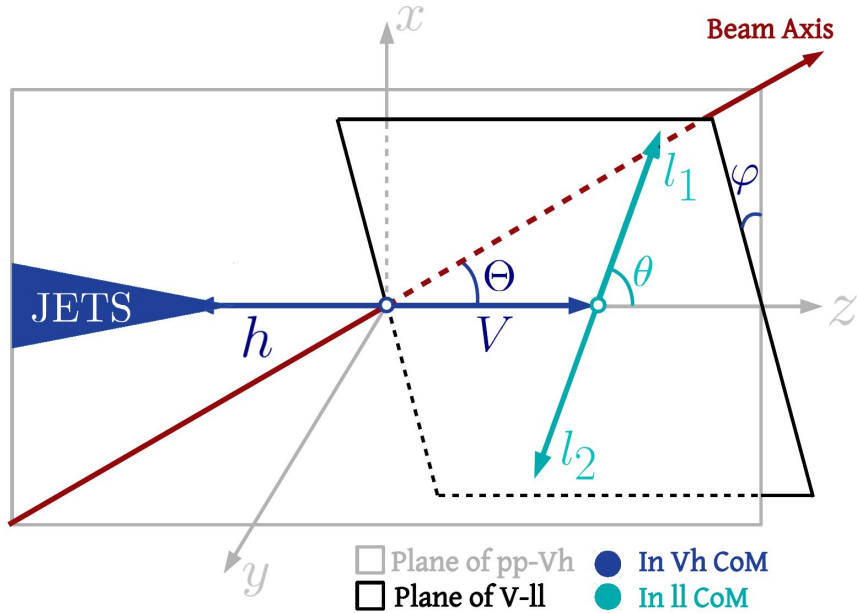


Top-Down approach

1. Wilson Coefficients determined in terms of new physics parameters
2. UV-complete Lagrangian must be known



Vh production at pp colliders



[SB, Gupta, Reiness, Seth, Spannowsky, 2020 \[JHEP 09 \(2020\) 170\]](#)

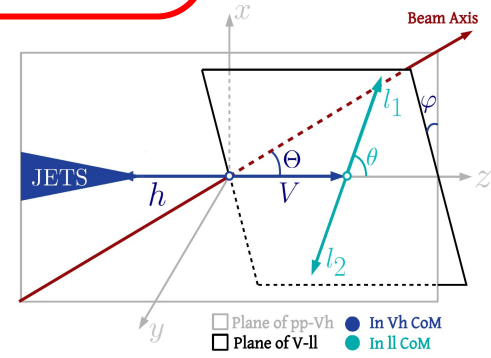
Vh production at pp colliders



- φ , Θ and $\{x, y, z\}$ in Vh CoM frame (z identified as direction of V-boson; y identified as normal to the plane of V and beam axis; x defined to complete the right-handed set), θ in V CoM frame
- Q: How much differential information can one extract from this process?
- For three body phase space, $3 \times 3 - 4 = 5$ kinematic variables completely define final state
- Barring boost factor, the variables are \sqrt{s} , Θ , θ , φ

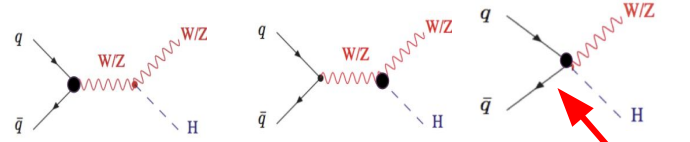
$$\begin{aligned}
 f_{LL} &= S_{\Theta}^2 S_{\theta}^2, \\
 f_{TT}^1 &= C_{\Theta} C_{\theta}, \\
 f_{TT}^2 &= (1 + C_{\Theta}^2)(1 + C_{\theta}^2), \\
 f_{LT}^1 &= C_{\varphi} S_{\Theta} S_{\theta}, \\
 f_{LT}^2 &= C_{\varphi} S_{\Theta} S_{\theta} C_{\Theta} C_{\theta}, \\
 \tilde{f}_{LT}^1 &= S_{\varphi} S_{\Theta} S_{\theta}, \\
 \tilde{f}_{LT}^2 &= S_{\varphi} S_{\Theta} S_{\theta} C_{\Theta} C_{\theta}, \\
 f_{TT'} &= C_{2\varphi} S_{\Theta}^2 S_{\theta}^2, \\
 \tilde{f}_{TT'} &= S_{2\varphi} S_{\Theta}^2 S_{\theta}^2,
 \end{aligned}$$

Many angular distributions testable at the LHC



SB, Gupta, Reiness, Seth, Spannowsky, 2020 [JHEP 09 (2020) 170]

Zh and Wh production at the LHC



SM scaling
k-framework

Diagram not
in the SM

$$\Delta\mathcal{L}_6 \supset \delta\hat{g}_{WW}^h \frac{2m_W^2}{v} hW^{+\mu}W_{\mu}^- + \delta\hat{g}_{ZZ}^h \frac{2m_Z^2}{v} h \frac{Z^\mu Z_\mu}{2} + \delta g_Q^W (W_\mu^+ \bar{u}_L \gamma^\mu d_L + h.c.)$$

$$+ \delta g_L^W (W_\mu^+ \bar{\nu}_L \gamma^\mu e_L + h.c.) + g_{WL}^h \frac{h}{v} (W_\mu^+ \bar{\nu}_L \gamma^\mu e_L + h.c.)$$

$$+ g_{WQ}^h \frac{h}{v} (W_\mu^+ \bar{u}_L \gamma^\mu d_L + h.c.) + \sum_f (\delta g_f^Z Z_\mu \bar{f} \gamma^\mu f + \sum_f g_{Zf}^h \frac{h}{v} Z_\mu \bar{f} \gamma^\mu f)$$

Contact interaction; no
propagator; Energy growth

$$+ \kappa_{WW} \frac{h}{v} W^{+\mu\nu} W_{\mu\nu}^- + \tilde{\kappa}_{WW} \frac{h}{v} W^{+\mu\nu} \tilde{W}_{\mu\nu}^- + \kappa_{ZZ} \frac{h}{2v} Z^{\mu\nu} Z_{\mu\nu}$$

CP-even new Lorentz structure
(angular deformation)

CP-odd new
Lorentz
structure
(angular
deformation)

$$+ \tilde{\kappa}_{ZZ} \frac{h}{2v} Z^{\mu\nu} \tilde{Z}_{\mu\nu} + \kappa_{Z\gamma} \frac{h}{v} A^{\mu\nu} Z_{\mu\nu} + \tilde{\kappa}_{Z\gamma} \frac{h}{v} A^{\mu\nu} \tilde{Z}_{\mu\nu} + \delta\hat{g}_{bb}^h \frac{\sqrt{2}m_b}{v} h b \bar{b}$$

$$+ \kappa_{\gamma\gamma} \frac{h}{v} A^{\mu\nu} A_{\mu\nu}$$

Deformations written in broken phase after symmetry breaking

High-energy primaries

1. The four channels, viz., Zh , $W^\pm h$, W^+W^- and $W^\pm Z$ can be expressed (at high energies) respectively as $G^0 h$, $G^\pm h$, G^+G^- and $G^\pm G^0$ and the Higgs field can be written as

$$\begin{pmatrix} G^+ \\ \frac{h+iG^0}{2} \end{pmatrix}$$

2. These four final states are **intrinsically connected by gauge symmetry** even though they are very different from a collider physics point of view
3. With the **Goldstone boson equivalence theorem**, it is possible to compute amplitudes for various components of the Higgs in the unbroken phase
4. **Full $SU(2)$ theory is manifest** [[Franceschini, Panico, Pomarol, Riva, Wulzer, 2017](#)]

High-energy primaries: the EFT operators at play

Warsaw basis

$$\mathcal{O}_L^{(3)} = (\bar{Q}_L \sigma^a \gamma^\mu Q_L) (iH^\dagger \sigma^a \overleftrightarrow{D}_\mu H)$$

$$\mathcal{O}_L = (\bar{Q}_L \gamma^\mu Q_L) (iH^\dagger \overleftrightarrow{D}_\mu H)$$

$$\mathcal{O}_R^u = (\bar{u}_R \gamma^\mu u_R) (iH^\dagger \overleftrightarrow{D}_\mu H)$$

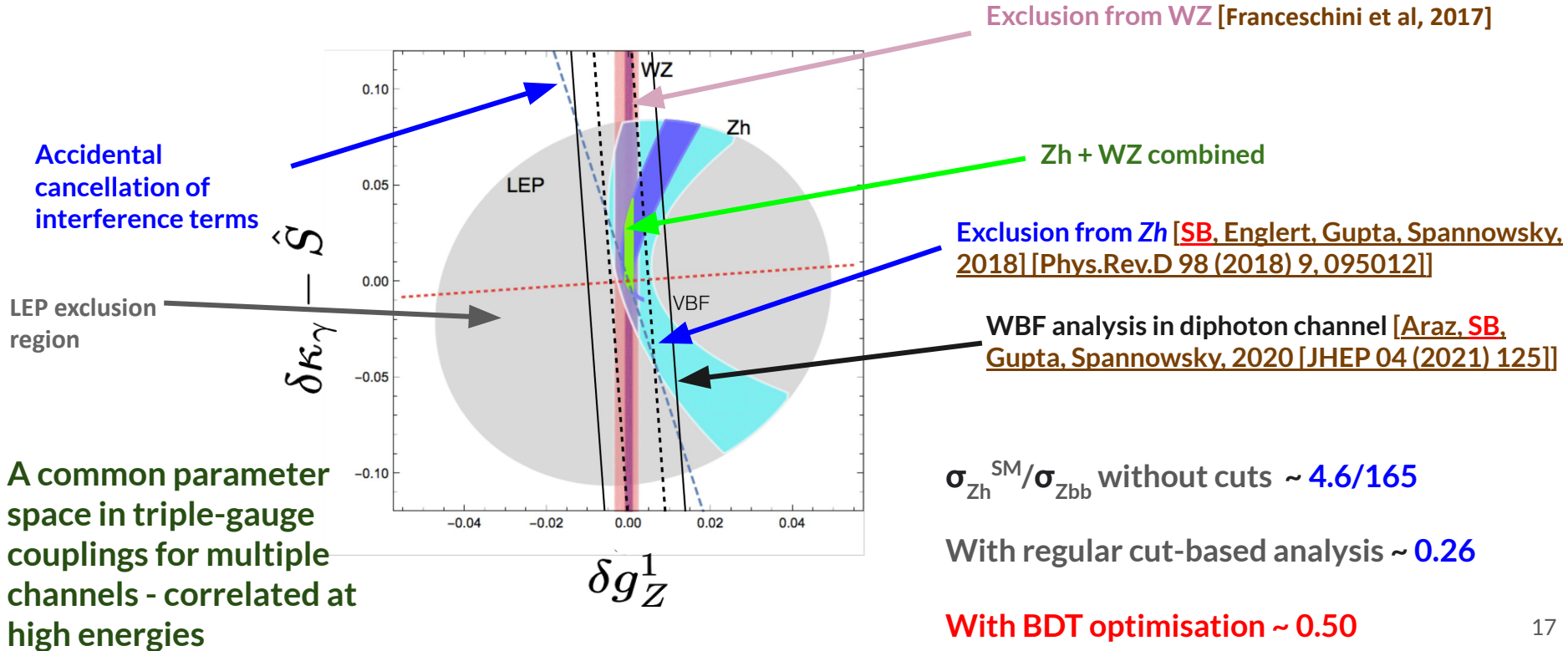
$$\mathcal{O}_R^d = (\bar{d}_R \gamma^\mu d_R) (iH^\dagger \overleftrightarrow{D}_\mu H)$$

Dimension-6 operators contributing to the high energy diboson production channels [Franceschini, Panico, Pomarol, Riva, Wulzer, 2017]

Relating the high-energy primaries with the Warsaw basis operators

We are dealing with four channels and there are only four independent couplings at play at high energies - coincidence!

Differential in energy: constraining the contact terms



Differential in energy: constraining the contact terms

	Our 100 TeV Projection	Our 14 TeV projection	LEP Bound
δg_{UU}^Z	$\pm 0.0003 (\pm 0.0001)$	$\pm 0.002 (\pm 0.0007)$	-0.0026 ± 0.0032
δg_{dL}^Z	$\pm 0.0003 (\pm 0.0001)$	$\pm 0.003 (\pm 0.001)$	0.0023 ± 0.002
δg_{uR}^Z	$\pm 0.0005 (\pm 0.0002)$	$\pm 0.005 (\pm 0.001)$	-0.0036 ± 0.0070
δg_{dR}^Z	$\pm 0.0015 (\pm 0.0006)$	$\pm 0.016 (\pm 0.005)$	0.016 ± 0.0104
δg_1^Z	$\pm 0.0005 (\pm 0.0002)$	$\pm 0.005 (\pm 0.001)$	$-0.009^{+0.043}_{-0.042}$
$\delta \kappa_\gamma$	$\pm 0.0035 (\pm 0.0015)$	$\pm 0.032 (\pm 0.009)$	$-0.016^{+0.085}_{-0.096}$
\hat{S}	$\pm 0.0035 (\pm 0.0015)$	$\pm 0.032 (\pm 0.009)$	0.0004 ± 0.0007
W	$\pm 0.0004 (\pm 0.0002)$	$\pm 0.003 (\pm 0.001)$	-0.0003 ± 0.0006
Y	$\pm 0.0035 (\pm 0.0015)$	$\pm 0.032 (\pm 0.009)$	0.0000 ± 0.0006

Single parameter fits
from Zh

[SB, Englert, Gupta, Spannowsky,
2018, 2019]

Directions from VBF, Zh, Wh, and WZ

[Araz, SB, Gupta, Spannowsky, 2020]

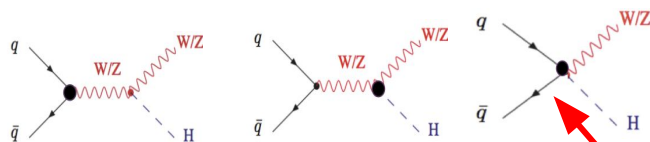
$$|(-0.04 c_Q^1 + 1.4 c_Q^{(3)} + 0.1 c_{uR} - 0.03 c_{dR})\xi| < 0.003 \quad [VBF]$$

$$|(-0.18 c_Q^1 + 1.3 c_Q^{(3)} + 0.3 c_{uR} - 0.1 c_{dR})\xi| < 0.0005 \quad [Zh]$$

What about the W^+W^- direction? $|c_Q^{(3)}\xi| < 0.0004 \quad [Wh]$

$$-0.0004 < c_Q^{(3)}\xi < 0.0003 \quad [WZ]$$

Zh and Wh production at the LHC



SM scaling
k-framework

Diagram not
in the SM

$$\Delta\mathcal{L}_6 \supset \delta\hat{g}_{WW}^h \frac{2m_W^2}{v} hW^{+\mu}W_{\mu}^- + \delta\hat{g}_{ZZ}^h \frac{2m_Z^2}{v} h \frac{Z^{\mu}Z_{\mu}}{2} + \delta g_Q^W (W_{\mu}^+ \bar{u}_L \gamma^{\mu} d_L + h.c.)$$

$$+ \delta g_L^W (W_{\mu}^+ \bar{\nu}_L \gamma^{\mu} e_L + h.c.) + g_{WL}^h \frac{h}{v} (W_{\mu}^+ \bar{\nu}_L \gamma^{\mu} e_L + h.c.)$$

$$+ g_{WQ}^h \frac{h}{v} (W_{\mu}^+ \bar{u}_L \gamma^{\mu} d_L + h.c.) + \sum_f (\delta g_f^Z) Z_{\mu} \bar{f} \gamma^{\mu} f + \sum_f g_{Zf}^h \frac{h}{v} Z_{\mu} \bar{f} \gamma^{\mu} f$$

Contact interaction; no
propagator; Energy growth

$$+ \kappa_{WW} \frac{h}{v} W^{+\mu\nu} W_{\mu\nu}^- + \tilde{\kappa}_{WW} \frac{h}{v} W^{+\mu\nu} \tilde{W}_{\mu\nu}^- + \kappa_{ZZ} \frac{h}{2v} Z^{\mu\nu} Z_{\mu\nu}$$

CP-even new Lorentz structure
(angular deformation)

CP-odd new
Lorentz
structure
(angular
deformation)

$$+ \tilde{\kappa}_{ZZ} \frac{h}{2v} Z^{\mu\nu} \tilde{Z}_{\mu\nu} + \kappa_{Z\gamma} \frac{h}{v} A^{\mu\nu} Z_{\mu\nu} + \tilde{\kappa}_{Z\gamma} \frac{h}{v} A^{\mu\nu} \tilde{Z}_{\mu\nu} + \delta\hat{g}_{bb}^h \frac{\sqrt{2}m_b}{v} hb\bar{b}$$

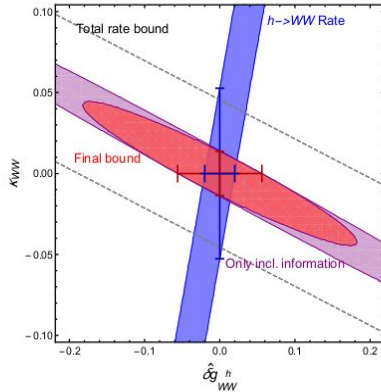
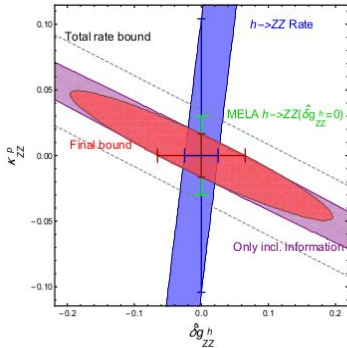
$$+ \kappa_{\gamma\gamma} \frac{h}{v} A^{\mu\nu} A_{\mu\nu}$$

Deformations written in broken phase after symmetry breaking

Differential in angles: constraining the angular terms

- Method of moments used to constrain the other couplings
- We obtain **percent level bounds on κ_{ZZ} and in the $(\kappa_{ZZ}, \delta\hat{g}_{ZZ}^h)$ plane**
- Competitive and complementary bounds to previous analyses
- Independent bound on the **CP-odd couplings!**
 $|\tilde{\kappa}_{ZZ}^P| < 0.03$

- We obtain **percent level bounds on κ_{WW} and in the $(\kappa_{WW}, \delta\hat{g}_{WW}^h)$ plane**
- Competitive and complementary bounds to previous analyses
- Independent bound on the **CP-odd coupling,**
 $|\tilde{\kappa}_{WW}^P| < 0.04$



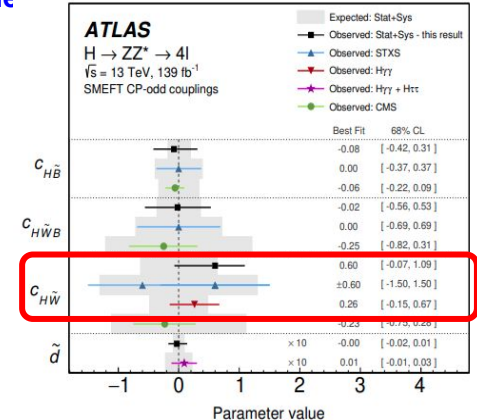
$$\tilde{\kappa}_{WW} = \frac{2v^2}{\Lambda^2} c_{H\tilde{W}}$$

$$\tilde{\kappa}_{ZZ} = \frac{2v^2}{\Lambda^2} (\cos^2 \theta_{WC} c_{H\tilde{W}} + \sin^2 \theta_{WC} c_{H\tilde{B}} + \sin \theta_{WC} \cos \theta_{WC} c_{H\tilde{W}B})$$

Assuming $\Lambda = 1 \text{ TeV}$, $c_{H\tilde{W}} < 0.33$ at 68% C.L. at HL-LHC!

We consider all operators simultaneously!
ATLAS considers one at a time

SB, Gupta, Reiness, Seth, Spannowsky, 2020 [JHEP 09 (2020) 170]



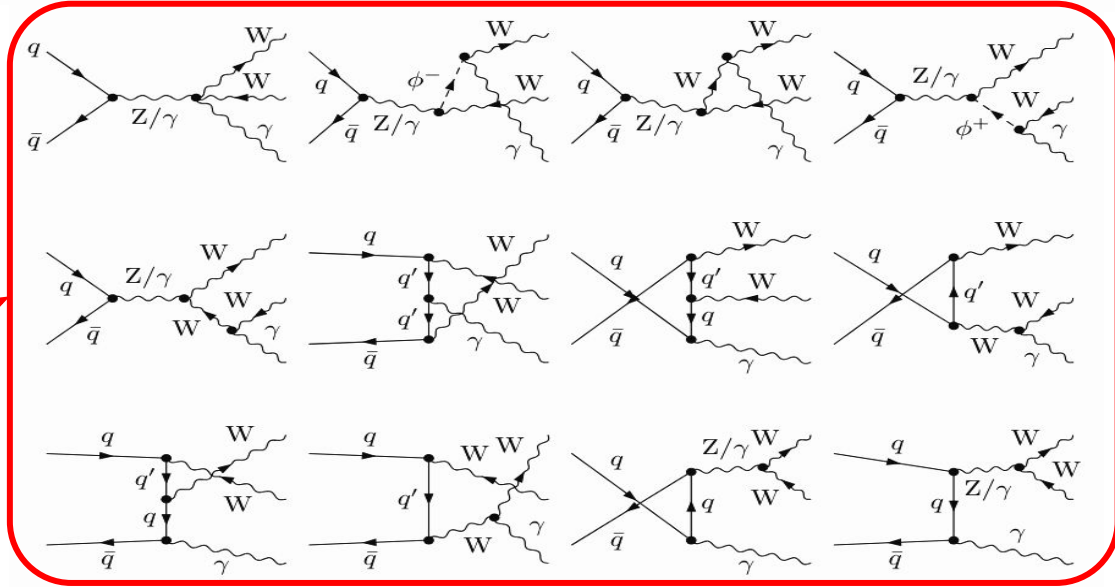
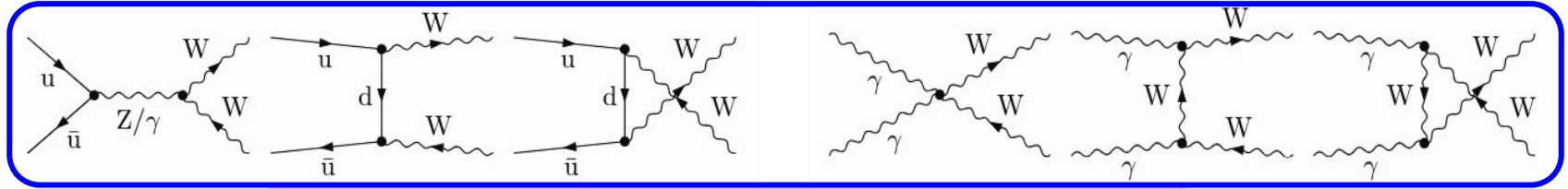
The W^+W^- channel

$$\begin{aligned}
 \Delta\mathcal{L}_{\text{BSM}} = & \delta g_{uL}^Z \left[Z^\mu \bar{u}_L \gamma_\mu u_L + \frac{\cos\theta_W}{\sqrt{2}} (W^{+\mu} \bar{u}_L \gamma_\mu d_L + \text{h.c.}) + \dots \right] + \delta g_{uR}^Z [Z^\mu \bar{u}_R \gamma_\mu u_R] \\
 & + \delta g_{dL}^Z \left[Z^\mu \bar{d}_L \gamma_\mu d_L - \frac{\cos\theta_W}{\sqrt{2}} (W^{+\mu} \bar{u}_L \gamma_\mu d_L + \text{h.c.}) + \dots \right] + \delta g_{dR}^Z [Z^\mu \bar{d}_R \gamma_\mu d_R] \\
 & + ig \cos\theta_W \delta g_1^Z [Z^\mu (W^{+\nu} W_{\mu\nu}^- - \text{h.c.}) + Z^{\mu\nu} W_\mu^+ W_\nu^- + \dots] \\
 & + ie\delta\kappa_\gamma [(A_{\mu\nu} - \tan\theta_W Z_{\mu\nu}) W^{+\mu} W^{-\nu} + \dots],
 \end{aligned}$$

with $Z_{\mu\nu} \equiv \hat{Z}_{\mu\nu} - iW_{[\mu}^+ W_{\nu]}^-$, $A_{\mu\nu} \equiv \hat{A}_{\mu\nu}$, $W_{\mu\nu}^\pm \equiv \hat{W}_{\mu\nu}^\pm \pm iW_{[\mu}^\pm (A + Z)_{\nu]}$, where $\hat{V}_{\mu\nu} = \partial_\mu V_\nu - \partial_\nu V_\mu$, and θ_W is the Weinberg angle

Electroweak corrections in W^+W^-

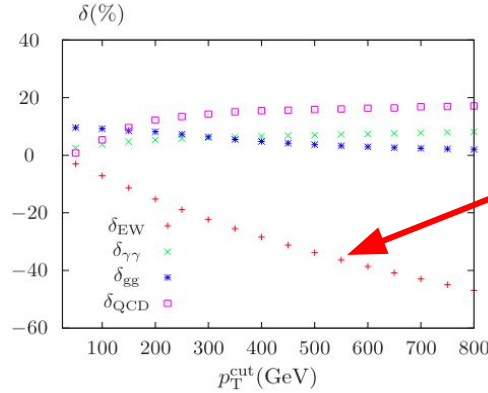
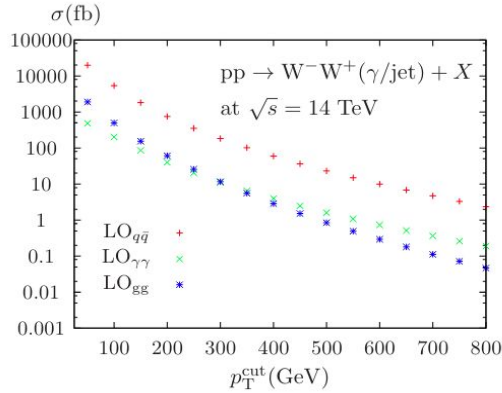
Leading order



[Bierweiler et al, 2012]

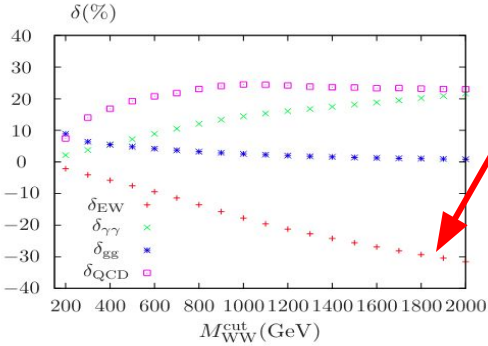
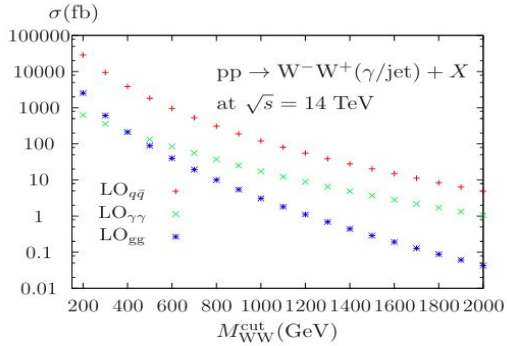
Real
bremsstrahlung
diagrams

Electroweak corrections in W^+W^-



Large (negative)
electroweak
corrections!

[Bierweiler et al, 2012]

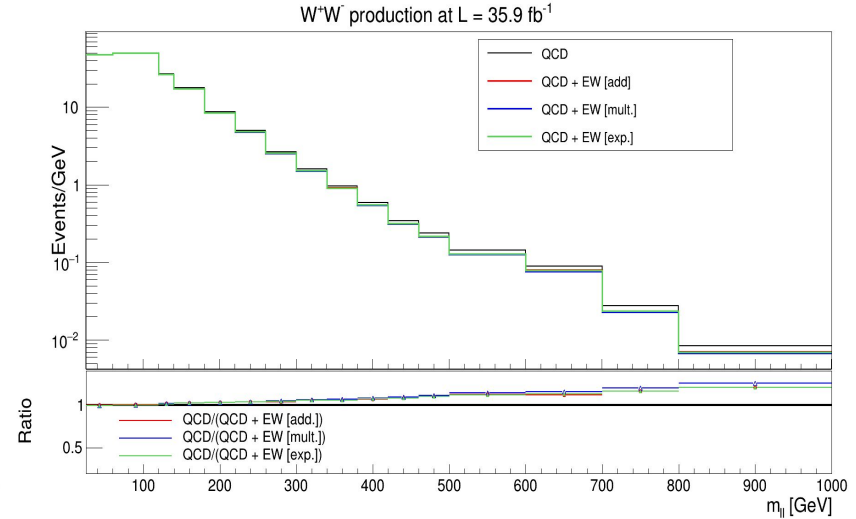
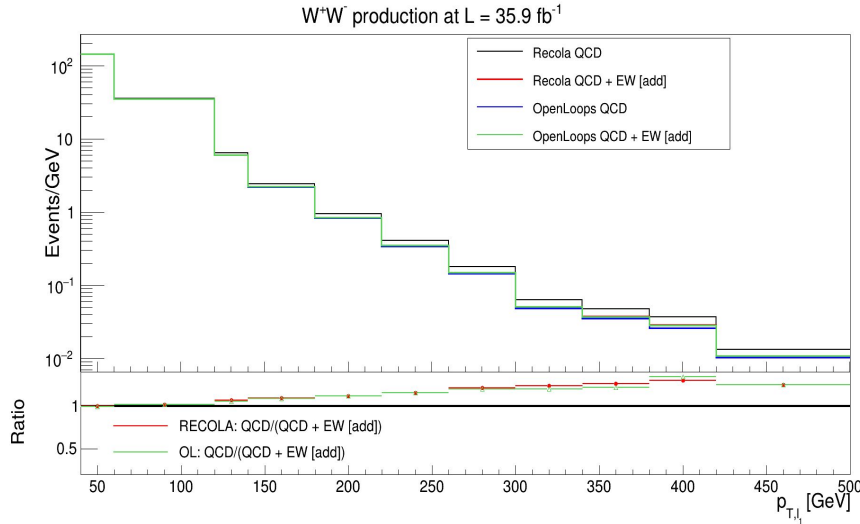


Event generation

$$pp \rightarrow W^+(l^+\nu)W^-(l^-\nu)$$

$$\mu_R^2 = \mu_F^2 = M_{\perp, W^+}^2 + M_{\perp, W^-}^2$$

[SB, Reichelt, Spannowsky, [arXiv:2406.15640](https://arxiv.org/abs/2406.15640), submitted to PRD]



Signal: SMEFT+SM interference; Backgrounds: Drell-Yan ($pp \rightarrow l^+l^-$), VZ , $t\bar{t} + tW$, $Wl\bar{l}$

χ^2 analysis

$$\chi^2 = \sum_i \sum_j \frac{[\mathcal{O}_{ij}^{\text{theo.}}(p) - \mathcal{O}_{ij}^{\text{exp., SM}}]^2}{\sigma_{ij}^2}$$

$$p = \delta g_{d_R}^Z, \delta g_{u_R}^Z, \delta g_{u_L}^Z, \text{ or } \delta g_{d_L}^Z$$

EFT coupling

$$\mathcal{O}_{ij}^{\text{theo.}}(p) = \mathcal{O}_{ij}^{\text{SM}} + p \times \mathcal{O}_{ij}^{\text{SMEFT}}$$

Our signal is the interference between SM and SMEFT

$$\sigma_{ij} = \sqrt{(\sigma_{ij,\text{stat.}}^{\text{exp.}})^2 + (\sigma_{ij,\text{stat.}}^{\text{theo.}})^2 + (\sigma_{ij,\text{syst.}}^{\text{exp.}})^2 + (\sigma_{ij,\text{syst.}}^{\text{theo.}})^2}$$

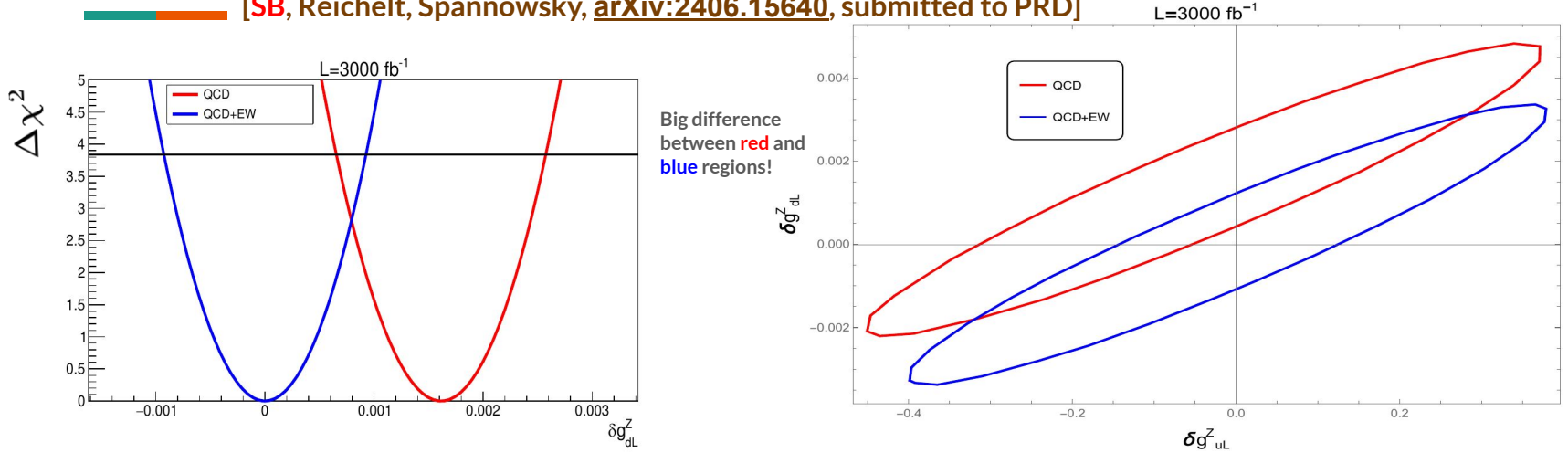
6 sub-categories: $e\mu - 0$, $e\mu - 1$, $ee - 0$, $ee - 1$, $\mu\mu - 0$, and $\mu\mu - 1$
'0' and '1' refer to the jet multiplicity

Theo. calculated at either SM@NLO-QCD+approximate-NLO-EW + SMEFT@LO or SM@NLO-QCD + SMEFT@LO

Exp. calculated at SM@NLO-QCD+approximate-NLO-EW

Results (95% C.L. bounds) - 1 and 2 parameter fits

[SB, Reichelt, Spannowsky, [arXiv:2406.15640](https://arxiv.org/abs/2406.15640), submitted to PRD]

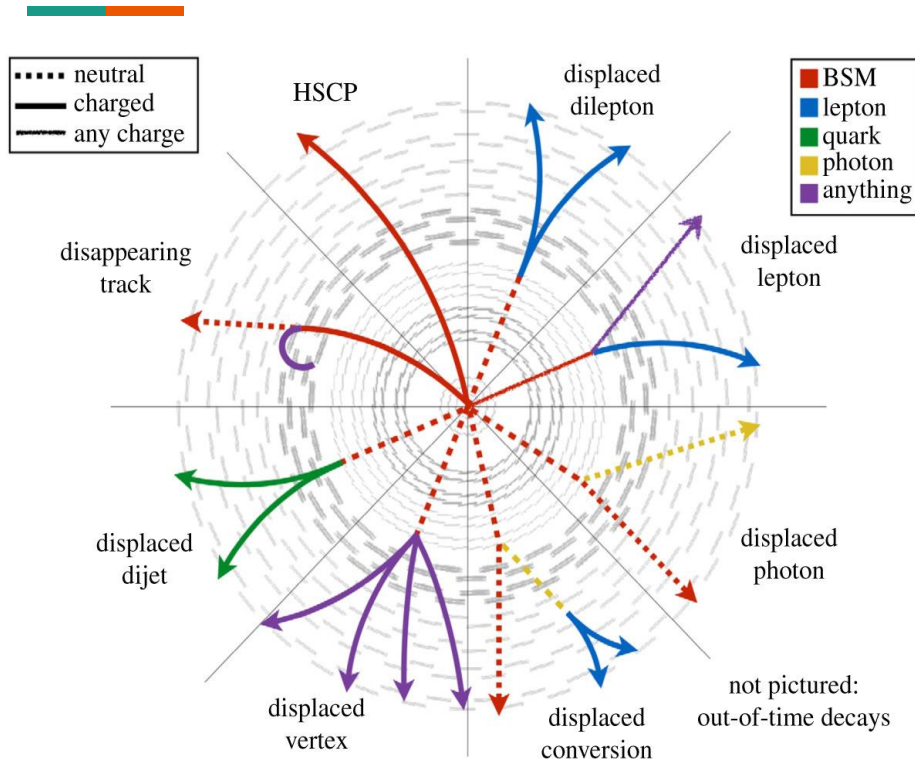


Coupling	QCD: $\mathcal{L} = 300 \text{ fb}^{-1}$	QCD+EW: $\mathcal{L} = 300 \text{ fb}^{-1}$	QCD: $\mathcal{L} = 3 \text{ ab}^{-1}$	QCD+EW: $\mathcal{L} = 3 \text{ ab}^{-1}$
δg_{dR}^Z	[-0.2744, 0.0531]	[-0.1569, 0.1569]	[-0.1611, -0.0421]	[-0.0567, 0.0567]
δg_{uP}^Z	[-0.0180, 0.0818]	[-0.0474, 0.0474]	[0.0111, 0.0463]	[-0.0167, 0.0167]
δg_{dL}^Z	[-0.0008, 0.0039]	[-0.0023, 0.0023]	[0.0006, 0.0026]	[-0.0010, 0.0010]
δg_{uL}^Z	[-0.3910, 0.0927]	[-0.2383, 0.2383]	[-0.2969, -0.0702]	[-0.1104, 0.1104]



Unconventional signatures

Long-Lived Particles: Search topologies



Roeck, 2019

Many models give rise to such signatures; example: RPV SUSY, AMSB SUSY, gauge-mediated SUSY, split SUSY, Hidden Valley models, dark QED, ALPs, and more.

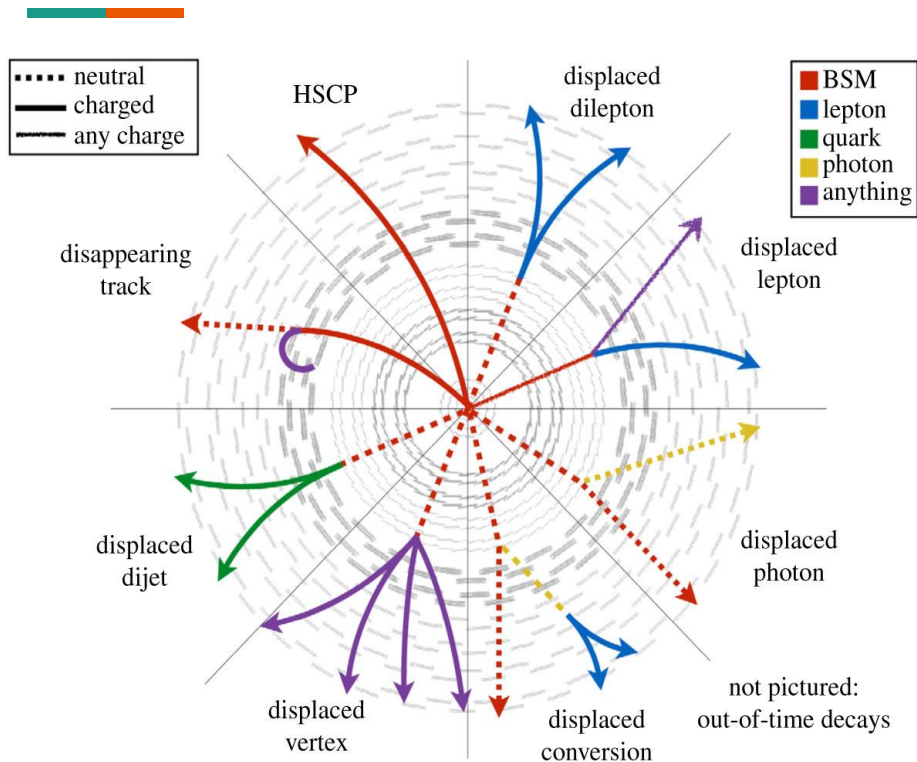
All of these searches require dedicated algorithms, detector modifications/additions, etc.

Long-Lived Particles: What's special?

1. Much reduced phase-space resulting from **small mass splitting** between LLP and one of its decay products.
2. **Suppressed coupling** controlling the dominant decay.
3. Traditional ways of reconstructing particles are inefficient.
4. Not trivial to perform fast detector simulation.
5. **Necessity for dedicated triggers:** Novel triggers can include **Displaced vertex triggers**, **MET triggers**, **Delayed Decay triggers** (example: utilising timing information), **Unusual topology triggers** (examples: multiple displaced vertices, asymmetric energy distributions, non-pointing photons), **Customised trigger algorithms** (information from multiple detector subsystems, such as tracking, calorimetry, timing), **Offline trigger rejection**

Disclaimer: I am not an expert on triggers by any means!

Long-Lived Particles: Search topologies



What's missing?

All of the LLP daughters move in the forward direction.

Are we exploring the full topology?

Long-Lived Particles: backward moving objects

1. We consider pair production of LLP, X
2. Daughters considered: light quark, q , or invisible particle, DM (may or may not satisfy dark matter properties)

3. We consider the following four possibilities

a) $X \rightarrow qq$ (Example: RPV decays of sleptons $\tilde{l} \rightarrow qq$) (2-body massless final state)

Quark initiated Drell-Yan process. **Scalar mother particle: no spin correlation!**

b) $X \rightarrow qqq$ (Example: RPV decays of sleptons $\tilde{\chi}_1^0 \rightarrow qq$) (3-body massless final state)

Quark initiated. **Effects of spin correlation may not be negligible!**

c) $X \rightarrow qDM$ (Example: RPC decays of lightest sbottom $\tilde{b}_1 \rightarrow b\tilde{\chi}_1^0$) (2-body final state)

Gluon initiated.

d) $X \rightarrow qqDM$ (Example: RPC decay $\tilde{g} \rightarrow qq\tilde{\chi}_1^0$) (3-body final state)

Gluon initiated.

Long-Lived Particles: backward moving objects

1. Signatures seen: multi-jets or multi-jets + MET
2. To exploit the full power of spin correlations, we consider X as a fermion for the 3-body decays
3. Any bias introduced by choice of prototype simulation on dynamics of the model?

Compare results of full simulation with those assuming no dynamics in production ($\mathcal{M} = 1$)

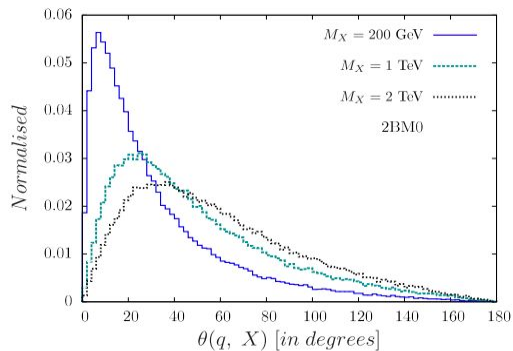
Helps in realising if results are mostly kinematics driven or not.

For this reason, we choose three distinct values of $M_{X'}$ and for each $M_{X'}$ two M_{DM}

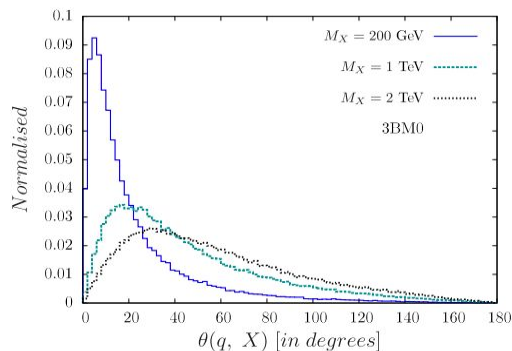
All simulations performed at parton level for 14 TeV LHC

4. $\beta (= p/E) = 0$ refers to the scenario when particle comes to a standstill after traversing a distance; example stopped R-hadron

Long-Lived Particles: angular separation (mother, daughter)

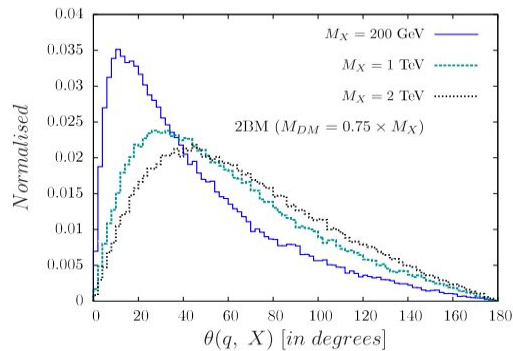


(a)

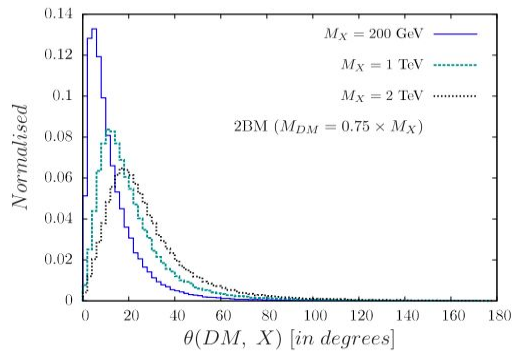


(b)

Angle θ between the direction of X and the massless daughter (one of the quarks, q) or the massive daughter

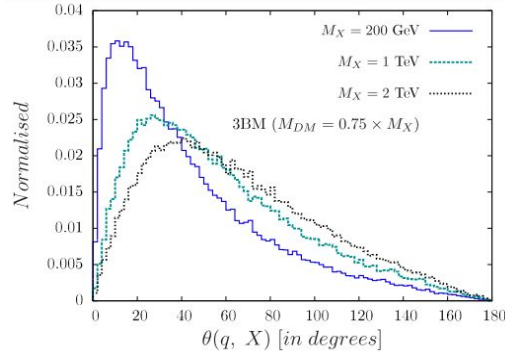


(c)

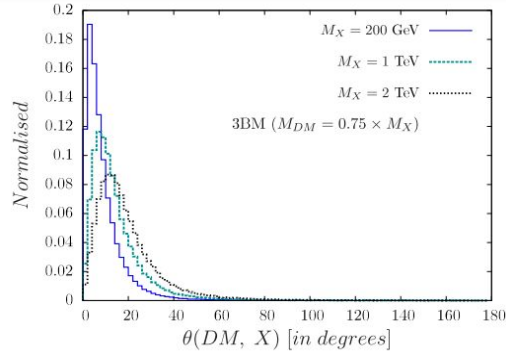


(d)

Long-Lived Particles: angular separation (mother, daughter)

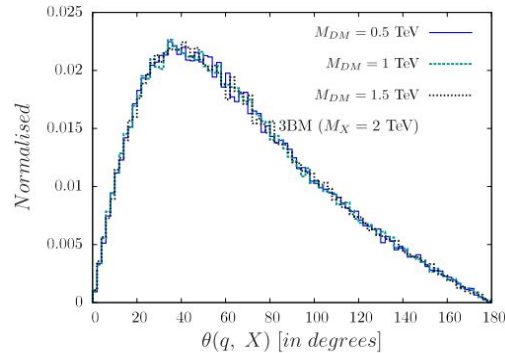


(e)

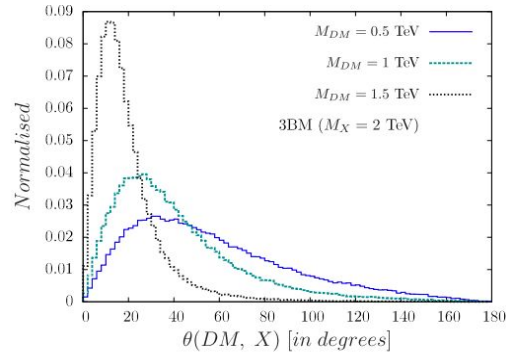


(f)

Angle θ between the direction of X and the massless daughter (one of the quarks, q) or the massive daughter

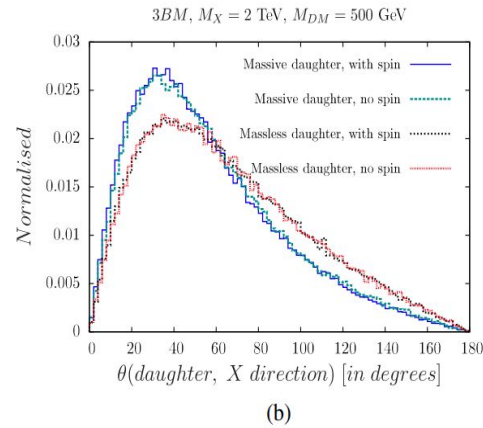
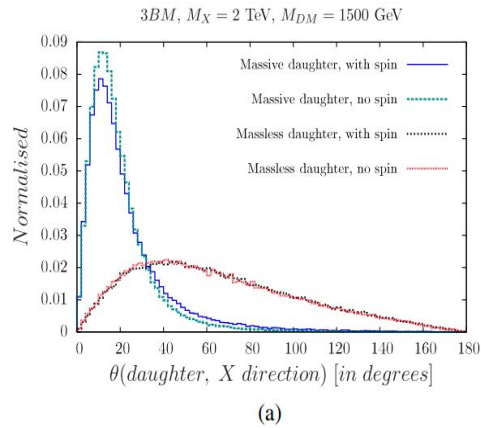


(g)



(h)

Long-Lived Particles: angular separation (effect of spin correlation)

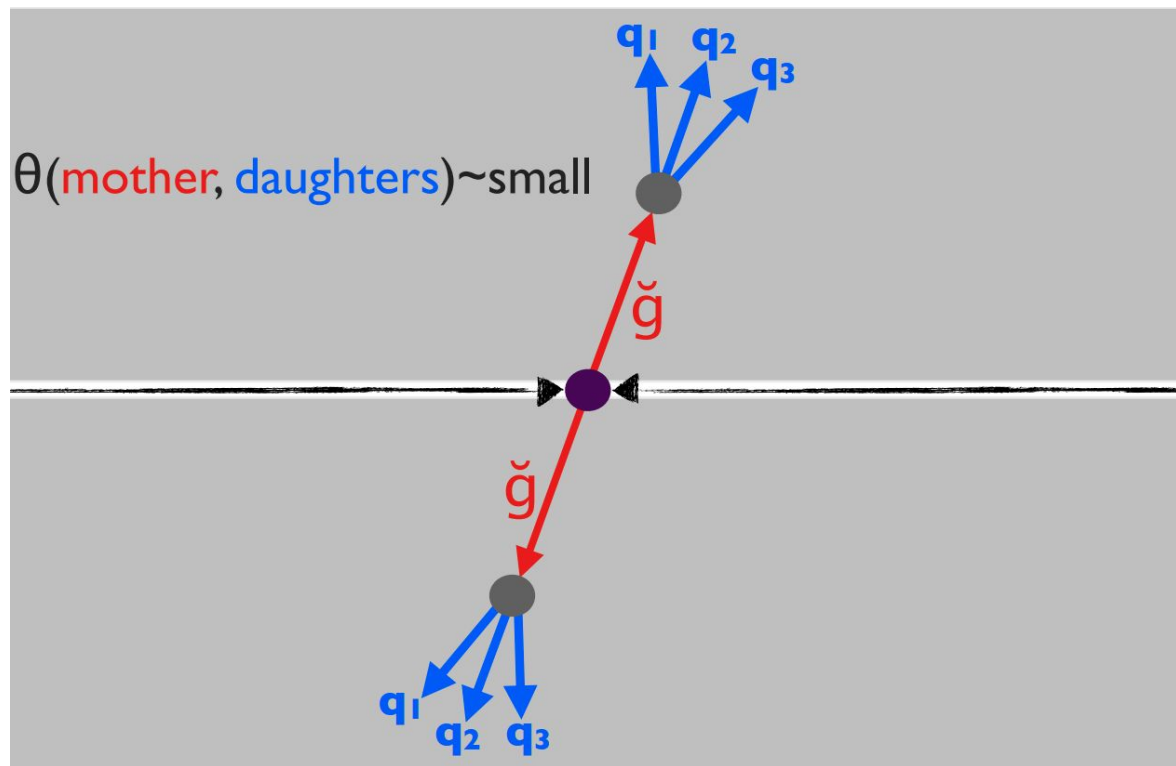


Angle θ between the direction of X and the massless daughter (one of the quarks, q) or the massive daughter

Spin-correlations preserved using MG5_aMC@NLO simulations

Spin averaging is a fairly good approximation!

Long-Lived Particles: backward moving objects

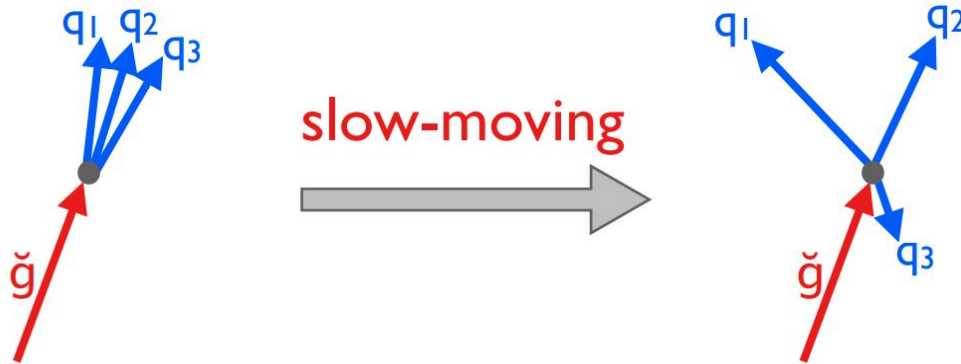


Usual displaced jets signatures!

Long-Lived Particles: backward moving objects

If \tilde{g} is heavy \rightarrow slow moving particle $\beta < 1$

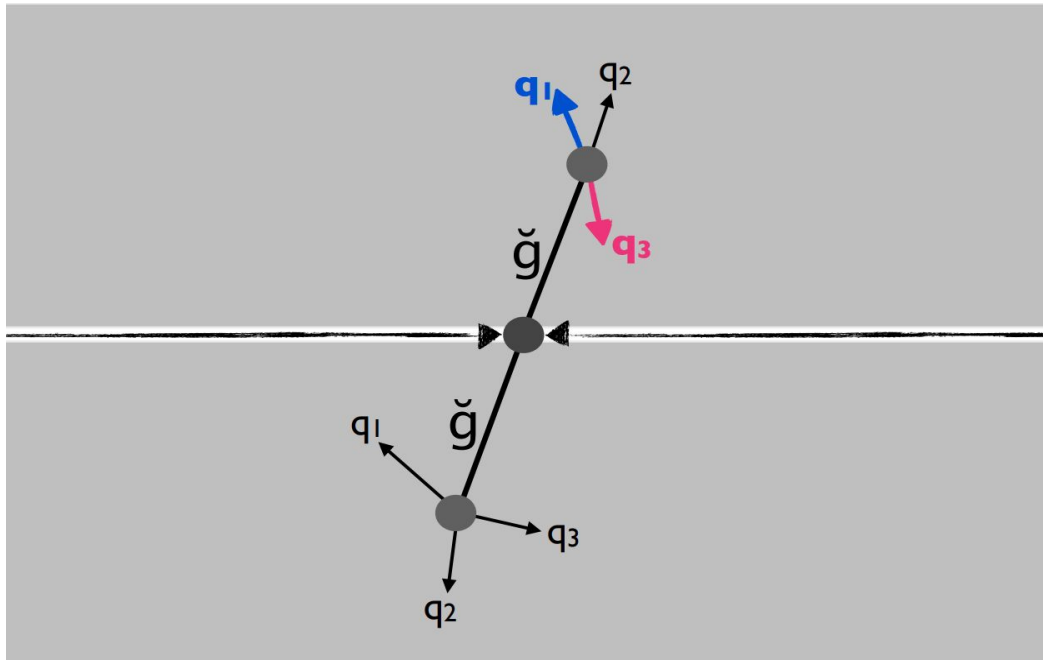
Decay products no longer collimated; $\theta(\text{mother}, \text{daughter})$ can be big



Picture courtesy: Swagata Mukherjee

Fraction of events with backward moving objects increases with decreasing β

Long-Lived Particles: **non-pointing** and **backward** moving objects



Picture courtesy: Swagata Mukherjee

How often at least one daughter non-pointing/backward moving?

$$\tilde{g}(\rightarrow q_1 q_2 q_3) \tilde{g}(\rightarrow q_1 q_2 q_3)$$

$M_{\tilde{g}}$	$\beta(\text{mean}, \text{RMS})$	$\theta > 22.5^\circ$	$\theta > 45^\circ$	$\theta > 90^\circ$	$\theta > 135^\circ$
1 TeV	0.76, 0.15	99%	84%	33%	7%
2 TeV	0.62, 0.15	100%	98%	52%	12%

Major fraction non-pointing

Non-negligible fraction
backward moving

How often at least one daughter non-pointing/backward moving?

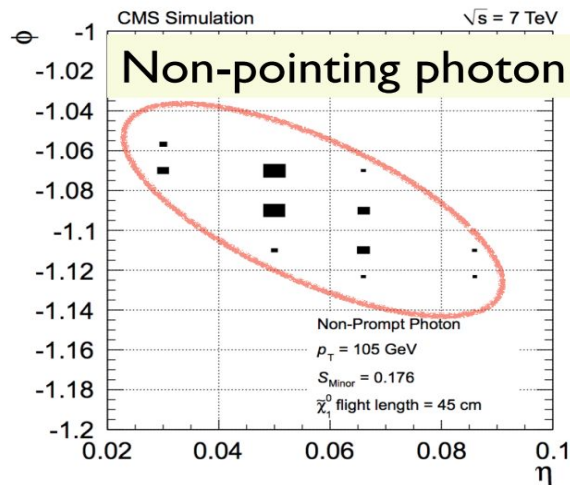
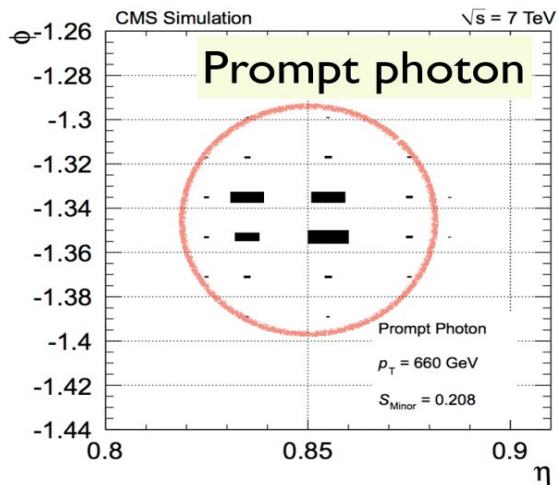
$$\tilde{l}(\rightarrow q_1 q_2) \tilde{l}(\rightarrow q_1 q_2)$$

$M_{\tilde{l}}$	$\beta(\text{mean}, \text{RMS})$	$\theta > 22.5^\circ$	$\theta > 45^\circ$	$\theta > 90^\circ$	$\theta > 135^\circ$
1 TeV	0.72, 0.15	99%	83%	28%	6%
2 TeV	0.60, 0.14	100%	97%	40%	8%

Major fraction non-pointing

Non-negligible fraction
backward moving

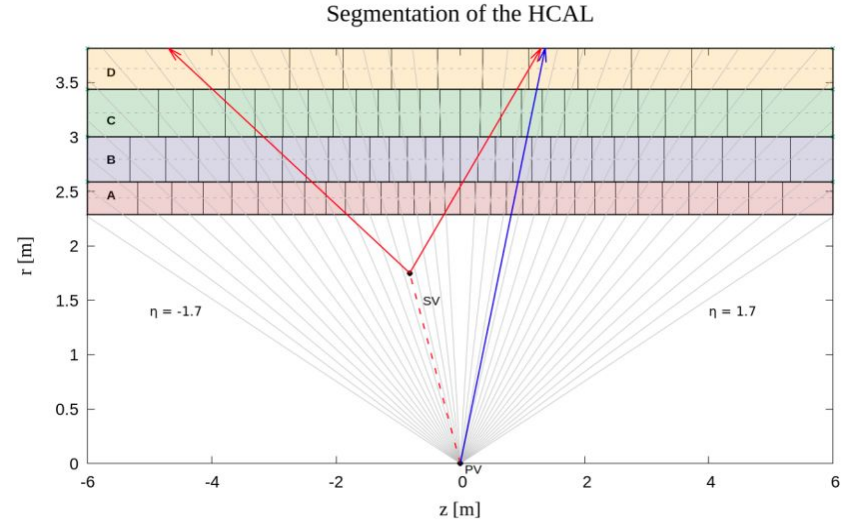
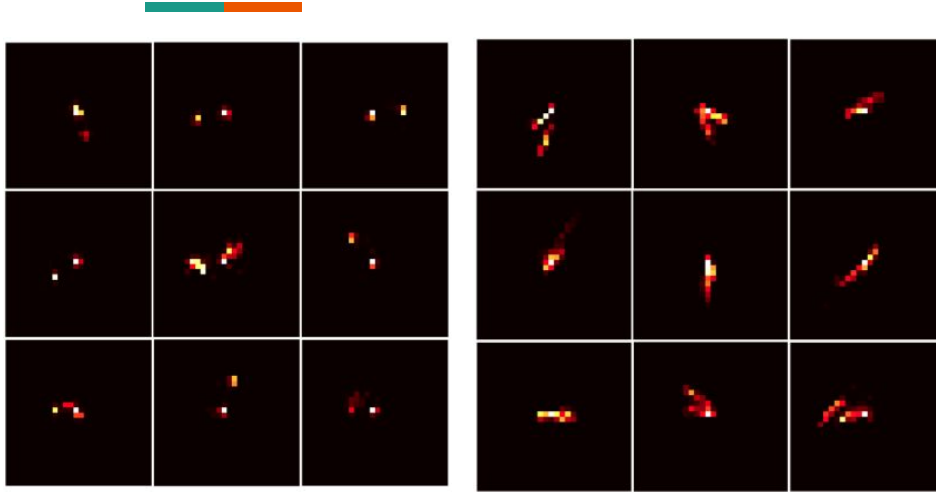
Non-pointing photons



- Non-pointing photons in ECAL already used in searches.
- Distinctive shower-shape for photon.

[arXiv:1212.1838](https://arxiv.org/abs/1212.1838)

Non-pointing jets



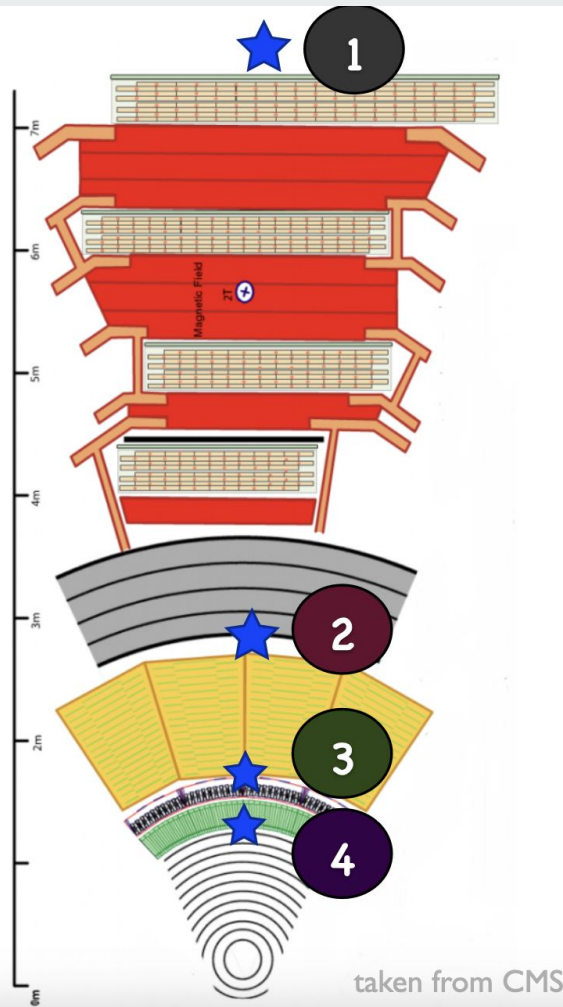
Standard particle contained in single η tower
Non-prompt particle shared between multiple η towers

- Z decaying to jets: no displacement (first)
- Z decaying to jets: transverse displacement of 200-220 cm (second)

[Bhattacharjee, Mukherjee, Sengupta, 2019](#)

Depending on lifetime of LLP, signature can be very different.

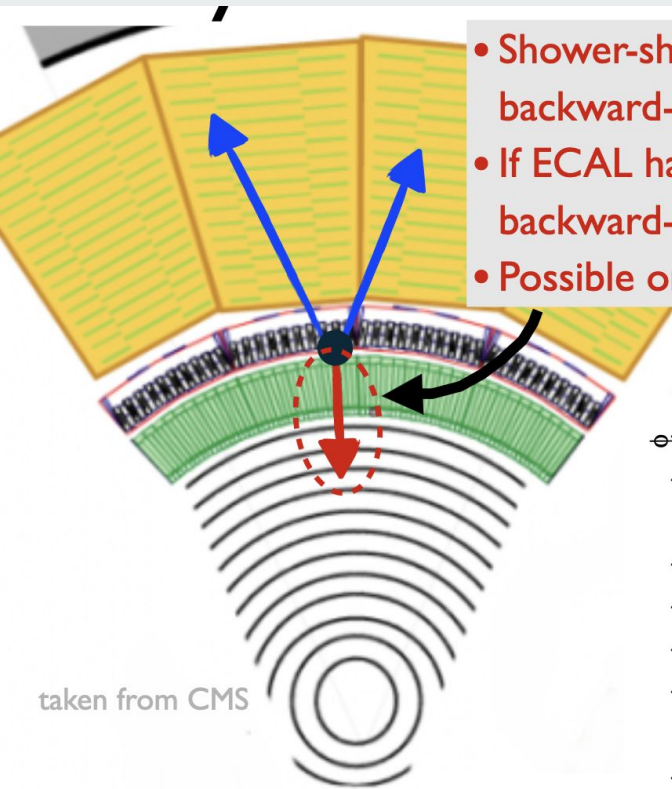
4 very different possible decay signatures!



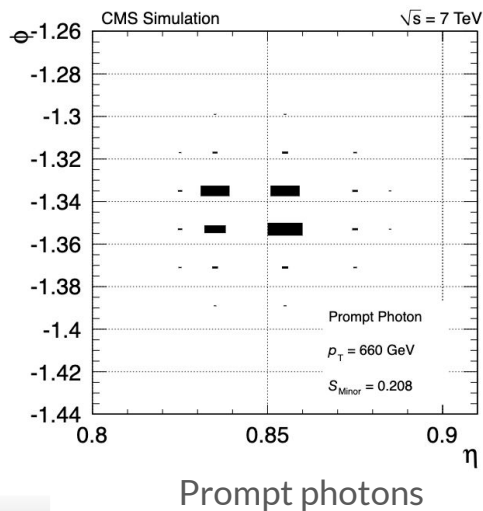
Decay outside ECAL

ECAL

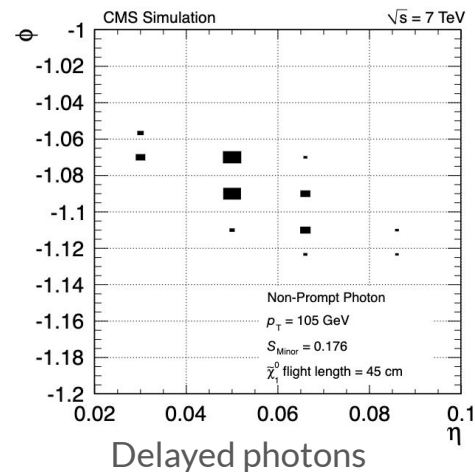
- Shower-shape expected to be different for backward-moving jet in ECAL
- If ECAL has longitudinal-segmentation, backward-moving jets can be identified in ECAL
- Possible only in sampling ECAL, e.g. ATLAS ECAL



taken from CMS



- Prompt EM objects from the collision enter the face of the crystal (since crystals face the interaction points)
- However these BMOs enter the ECAL crystals at an angle and hence difference in shower shapes
- Longitudinal segmentation of HGCal in HL-LHC will help



Summary



1. EFTs are important tools to understand the possible nature and type of new physics when resonance searches are not yielding results.
2. *Zh, Wh, WW and WZ* are important channels to disentangle various directions in the EFT space. They are intrinsically correlated.
3. Multiple dimensions come about from the various correlated EFT coefficients. Blind directions need to be broken.
4. Inclusion of electroweak corrections to the backgrounds can change the bounds on the SMEFT couplings considerably as what we may perceive to be a change owing to SMEFT deformations might be owing to higher-order corrections.
5. Backward moving objects give rise to a plethora of possible search strategies.



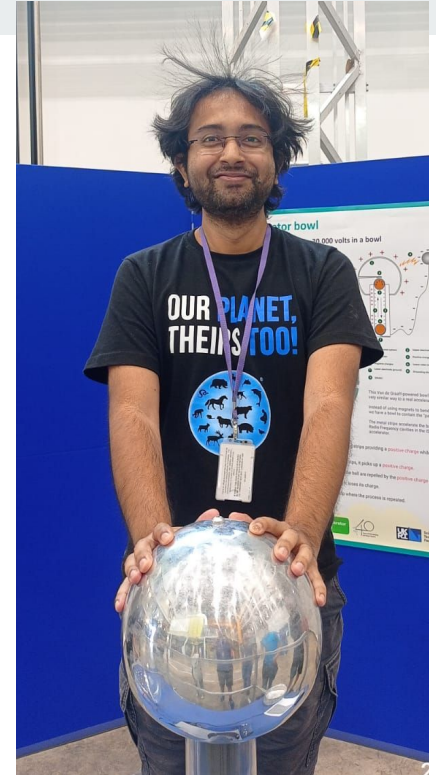
HOW 2024 volunteering for PPD



DarkSide cryogenic detector test setup at R115 cleanroom.

Thank you!!!

Please consider joining the [LHC EFT Working Group](#) to stay connected with the latest discussions between experimentalists and theorists on EFTs.



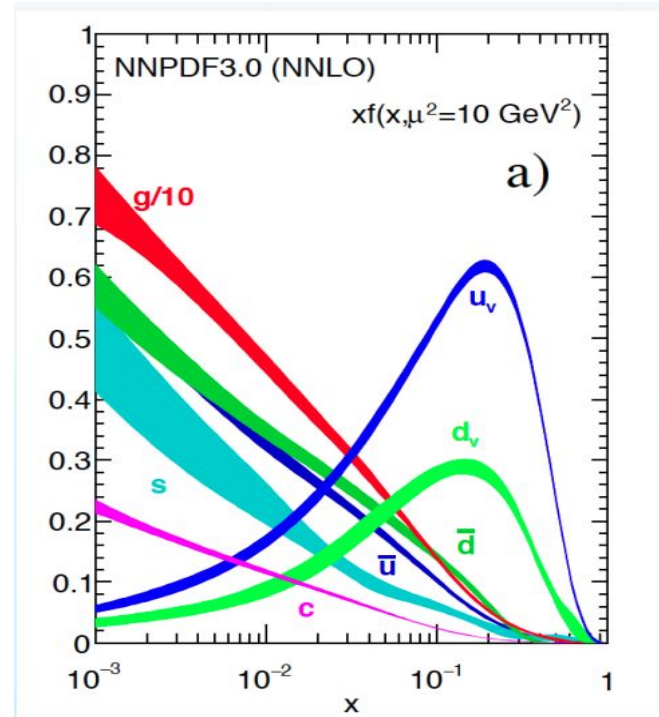
Van de Graaff generator at ISIS

Backup slides



Backup slides

LLPs from qq initiated initial states have larger \square



High-energy primaries

SILH basis	Warsaw basis
$\mathcal{O}_W = \frac{ig}{2}(H^\dagger \sigma^a \overleftrightarrow{D}^\mu H) D^\nu W_{\mu\nu}^a$	$\mathcal{O}_L^{(3)} = (\bar{Q}_L \sigma^a \gamma^\mu Q_L)(iH^\dagger \sigma^a \overleftrightarrow{D}_\mu H)$
$\mathcal{O}_B = \frac{ig'}{2}(H^\dagger \overleftrightarrow{D}^\mu H) \partial^\nu B_{\mu\nu}^a$	$\mathcal{O}_L = (\bar{Q}_L \gamma^\mu Q_L)(iH^\dagger \overleftrightarrow{D}_\mu H)$
$\mathcal{O}_{HW} = ig(D^\mu H)^\dagger \sigma^a (D^\nu H) W_{\mu\nu}^a$	$\mathcal{O}_R^u = (\bar{u}_R \gamma^\mu u_R)(iH^\dagger \overleftrightarrow{D}_\mu H)$
$\mathcal{O}_{HB} = ig(D^\mu H)^\dagger (D^\nu H) B_{\mu\nu}$	$\mathcal{O}_R^d = (\bar{d}_R \gamma^\mu d_R)(iH^\dagger \overleftrightarrow{D}_\mu H)$
$\mathcal{O}_{2W} = -\frac{1}{2}(D^\mu W_{\mu\nu}^a)^2$	
$\mathcal{O}_{2B} = -\frac{1}{2}(\partial^\mu B_{\mu\nu})^2$	

Dimension-6 operators contributing to the high energy longitudinal diboson production channels in the SILH and Warsaw bases [Franceschini, Panico, Pomarol, Riva, Wulzer, 2017]

$$a_u = 4 \frac{c_R^u}{\Lambda^2}, a_d = 4 \frac{c_R^d}{\Lambda^2}, a_q^{(1)} = 4 \frac{c_L^{(1)}}{\Lambda^2}, \text{ and } a_q^{(3)} = 4 \frac{c_L^{(3)}}{\Lambda^2}$$

Relating the high-energy primaries with the Warsaw basis operators

High-energy primaries

Amplitude	High-energy primaries
$\bar{u}_L d_L \rightarrow W_L Z_L, W_L h$	$\sqrt{2} a_q^{(3)}$
$\bar{u}_L u_L \rightarrow W_L W_L$ $\bar{d}_L d_L \rightarrow Z_L h$	$a_q^{(1)} + a_q^{(3)}$
$\bar{d}_L d_L \rightarrow W_L W_L$ $\bar{u}_L u_L \rightarrow Z_L h$	$a_q^{(1)} - a_q^{(3)}$
$\bar{f}_R f_R \rightarrow W_L W_L, Z_L h$	a_f

Amplitude	High-energy primaries
$\bar{u}_L d_L \rightarrow W_L Z_L, W_L h$	$\frac{g_{Z d_L d_L}^h - g_{Z u_L u_L}^h}{\sqrt{2}}$
$\bar{u}_L u_L \rightarrow W_L W_L$ $\bar{d}_L d_L \rightarrow Z_L h$	$g_{Z d_L d_L}^h$
$\bar{d}_L d_L \rightarrow W_L W_L$ $\bar{u}_L u_L \rightarrow Z_L h$	$g_{Z u_L u_L}^h$
$\bar{f}_R f_R \rightarrow W_L W_L, Z_L h$	$g_{Z f_R f_R}^h$

Vh and VV channels are entwined by symmetry and they constrain the same set of observables at High energies but may have different directions [Franceschini, Panico, Pomarol, Riva, Wulzer, 2017, SB, Gupta, Seth, Reiness, Spannowsky, 2020]

High-energy primaries

Amplitude	High-energy primaries	Low-energy primaries
$\bar{u}_L d_L \rightarrow W_L Z_L, W_L h$	$\sqrt{2} a_q^{(3)}$	$\sqrt{2} \frac{g^2}{m_W^2} [c_{\theta_W} (\delta g_{uL}^Z - \delta g_{dL}^Z)/g - c_{\theta_W}^2 \delta g_1^Z]$
$\bar{u}_L u_L \rightarrow W_L W_L$ $\bar{d}_L d_L \rightarrow Z_L h$	$a_q^{(1)} + a_q^{(3)}$	$-\frac{2g^2}{m_W^2} [Y_L t_{\theta_W}^2 \delta \kappa_\gamma + T_Z^{uL} \delta g_1^Z + c_{\theta_W} \delta g_{dL}^Z/g]$
$\bar{d}_L d_L \rightarrow W_L W_L$ $\bar{u}_L u_L \rightarrow Z_L h$	$a_q^{(1)} - a_q^{(3)}$	$-\frac{2g^2}{m_W^2} [Y_L t_{\theta_W}^2 \delta \kappa_\gamma + T_Z^{dL} \delta g_1^Z + c_{\theta_W} \delta g_{uL}^Z/g]$
$\bar{f}_R f_R \rightarrow W_L W_L, Z_L h$	a_f	$-\frac{2g^2}{m_W^2} [Y_{fR} t_{\theta_W}^2 \delta \kappa_\gamma + T_Z^{fR} \delta g_1^Z + c_{\theta_W} \delta g_{fR}^Z/g]$

Vh and VV channels are entwined by symmetry and they constrain the same set of observables at High energies but may have different directions [Franceschini, Panico, Pomarol, Riva, Wulzer, 2017, SB, Gupta, Reiness, Seth, Spannowsky, 2020]

Zh production (Helicity amplitude)

- For a $2 \rightarrow 2$ process $f(\sigma)\bar{f}(-\sigma) \rightarrow Zh$, the helicity amplitudes are given by

$$\mathcal{M}_\sigma^{\lambda=\pm} = \sigma \frac{1 + \sigma\lambda \cos\Theta}{\sqrt{2}} G_V \frac{m_V}{\sqrt{\hat{s}}} \left[\boxed{1} + \left(\frac{g_{Vf}^h}{g_f^V} + \hat{\kappa}_{VV} - i\lambda\hat{\tilde{\kappa}}_{VV} \right) \frac{\hat{s}}{2m_V^2} \right]$$

$$\mathcal{M}_\sigma^{\lambda=0} = -\frac{\sin\Theta}{2} G_V \left[\boxed{1} + \delta\hat{g}_{VV}^h + 2\hat{\kappa}_{VV} + \delta g_f^Z + \frac{g_{Vf}^h}{g_f^V} \left(-\frac{1}{2} + \frac{\hat{s}}{2m_V^2} \right) \right]$$

$$\begin{aligned} \hat{\kappa}_{WW} &= \kappa_{WW} \\ \hat{\kappa}_{ZZ} &= \kappa_{ZZ} + \frac{Q_f e}{g_f^Z} \kappa_{Z\gamma}, \\ \hat{\tilde{\kappa}}_{ZZ} &= \tilde{\kappa}_{ZZ} + \frac{Q_f e}{g_f^Z} \tilde{\kappa}_{Z\gamma} \end{aligned}$$

SB, Englert, Gupta, Spannowsky, 2018

- $\lambda = \pm 1$ and $\sigma = \pm 1$ are, respectively, the helicities of the Z-boson and initial-state fermions, $g_f^Z = g(T_3^f - Q_f s_{\theta_W}^2)/c_{\theta_W}$
- Leading SM is longitudinal ($\lambda = 0$), Leading effect of κ_{WW} , κ_{ZZ} , $\tilde{\kappa}_{ZZ}$ is in the transverse-longitudinal (LT) interference, LT term vanishes if we aren't careful

Vh production (Helicity amplitude)

- The differential cross-section for the process $pp \rightarrow Z(\ell^+ \ell^-)/W(\ell\nu)h(b\bar{b})$ is a differential in four variables, viz., $\frac{d\sigma}{dEd\Theta d\theta d\varphi}$
- The amplitude at the decay level can be written as

$$\mathcal{A}(\hat{s}, \Theta, \theta, \varphi) = \frac{-ig_\ell^V + \delta g_\ell^V}{\Gamma_V} \sum_\lambda \mathcal{M}_\sigma^\lambda(\hat{s}, \Theta) d_{\lambda,1}^{J=1}(\theta) e^{i\lambda\hat{\varphi}}$$

SB, Englert, Gupta, Spannowsky, 2018

- $d_{\pm 1,1}^{J=1} = \tau \frac{1 \pm \tau \cos \theta}{\sqrt{2}}$, $d_{0,1}^{J=1} = \sin \theta$ are the Wigner functions, τ is lepton helicity, Γ_V is the V-width and $g_f^Z = g(T_3^f - Q_f s_{\theta_W}^2)/c_{\theta_W}$ and $g_f^W = g/\sqrt{2}$
- $\hat{\varphi} \rightarrow$ azimuthal angle of positive helicity lepton, $\hat{\theta} \rightarrow$ its polar angle in Z-rest frame
- Polarisation of lepton is experimentally not accessible
 - $\mathcal{A}_0 \sim \sin \Theta \sin \theta$
 - $\mathcal{A}_+ \sim (1 + \cos \Theta)(1 + \cos \theta) e^{i\varphi}$
 - $\mathcal{A}_- \sim (1 - \cos \Theta)(1 - \cos \theta) e^{-i\varphi}$



Four directions in the EFT space (Warsaw Basis)

$$g_{Zu_Lu_L}^h = -\frac{g}{c_{\theta_W}} \frac{v^2}{\Lambda^2} (c_L^1 - c_L^3)$$

$$g_{Zd_Ld_L}^h = -\frac{g}{c_{\theta_W}} \frac{v^2}{\Lambda^2} (c_L^1 + c_L^3)$$

$$g_{Zu_Ru_R}^h = -\frac{g}{c_{\theta_W}} \frac{v^2}{\Lambda^2} c_R^u$$

$$g_{Zd_Rd_R}^h = -\frac{g}{c_{\theta_W}} \frac{v^2}{\Lambda^2} c_R^d$$



Four directions in the EFT space (SILH Basis)

$$g_{Zu_Lu_L}^h = \frac{g}{c_{\theta_W}} \frac{m_W^2}{\Lambda^2} (c_W + c_{HW} - c_{2W} - \frac{t_{\theta_W}^2}{3} (c_B + c_{HB} - c_{2B}))$$

$$g_{Zd_Ld_L}^h = -\frac{g}{c_{\theta_W}} \frac{m_W^2}{\Lambda^2} (c_W + c_{HW} - c_{2W} + \frac{t_{\theta_W}^2}{3} (c_B + c_{HB} - c_{2B}))$$

$$g_{Zu_Ru_R}^h = -\frac{4gs_{\theta_W}^2}{3c_{\theta_W}^3} \frac{m_W^2}{\Lambda^2} (c_B + c_{HB} - c_{2B})$$

$$g_{Zd_Rd_R}^h = \frac{2gs_{\theta_W}^2}{3c_{\theta_W}^3} \frac{m_W^2}{\Lambda^2} (c_B + c_{HB} - c_{2B})$$

Four directions in the EFT space (Higgs primaries)

$$g_{Zu_Lu_L}^h = 2\delta g_{Zu_Lu_L}^Z - 2\delta g_1^Z (g_f^Z c_{2\theta_W} + eQ s_{2\theta_W}) + 2\delta\kappa_\gamma g' Y_h \frac{s_{\theta_W}}{c_{\theta_W}^2}$$

$$g_{Zd_Ld_L}^h = 2\delta g_{Zd_Ld_L}^Z - 2\delta g_1^Z (g_f^Z c_{2\theta_W} + eQ s_{2\theta_W}) + 2\delta\kappa_\gamma g' Y_h \frac{s_{\theta_W}}{c_{\theta_W}^2}$$

$$g_{Zu_Ru_R}^h = 2\delta g_{Zu_Ru_R}^Z - 2\delta g_1^Z (g_f^Z c_{2\theta_W} + eQ s_{2\theta_W}) + 2\delta\kappa_\gamma g' Y_h \frac{s_{\theta_W}}{c_{\theta_W}^2}$$

$$g_{Zd_Rd_R}^h = 2\delta g_{Zd_Rd_R}^Z - 2\delta g_1^Z (g_f^Z c_{2\theta_W} + eQ s_{2\theta_W}) + 2\delta\kappa_\gamma g' Y_h \frac{s_{\theta_W}}{c_{\theta_W}^2}$$

Four directions in the EFT space (Universal model)

$$g_{Zu_Lu_L}^h = -\frac{g}{c_{\theta_W}} \left((c_{\theta_W}^2 + \frac{s_{\theta_W}^2}{3}) \delta g_1^Z + W + \frac{t_{\theta_W}^2}{3} (\hat{S} - \delta\kappa_\gamma - Y) \right)$$

$$g_{Zd_Ld_L}^h = \frac{g}{c_{\theta_W}} \left((c_{\theta_W}^2 - \frac{s_{\theta_W}^2}{3}) \delta g_1^Z + W - \frac{t_{\theta_W}^2}{3} (\hat{S} - \delta\kappa_\gamma - Y) \right)$$

$$g_{Zu_Ru_R}^h = -\frac{4gs_{\theta_W}^2}{3c_{\theta_W}^3} (\hat{S} - \delta\kappa_\gamma + c_{\theta_W}^2 \delta g_1^Z - Y)$$

$$g_{Zd_Rd_R}^h = \frac{2gs_{\theta_W}^2}{3c_{\theta_W}^3} (\hat{S} - \delta\kappa_\gamma + c_{\theta_W}^2 \delta g_1^Z - Y)$$

EFT space directions

- δg_f^Z and δg_{ZZ}^h → deviations in SM amplitude
- These do not grow with energy and are suppressed by $\mathcal{O}(m_Z^2/\hat{s})$ w.r.t. g_{Vf}^h
- Five directions: g_{Zf}^h with $f = u_L, u_R, d_L, d_R$ and g_{Wud}^h → only four operators in Warsaw basis
- Knowing proton polarisation is not possible and hence in reality there are two directions Also, upon only considering interference terms, we have

$$g_{\mathbf{u}}^Z = g_{Zu_L}^h + \frac{g_{u_R}^Z}{g_{u_L}^Z} g_{Zu_R}^h$$

$$g_{\mathbf{d}}^Z = g_{Zd_L}^h + \frac{g_{d_R}^Z}{g_{d_L}^Z} g_{Zd_R}^h \quad g_{\mathbf{p}}^Z = g_{\mathbf{u}}^Z + \frac{\mathcal{L}_d(\hat{s})}{\mathcal{L}_u(\hat{s})} g_{\mathbf{d}}^Z$$

$$g_{\mathbf{p}}^Z = g_{Zu_L}^h - 0.76 g_{Zd_L}^h - 0.45 g_{Zu_R}^h + 0.14 g_{Zd_R}^h - 0.14 \delta\kappa_\gamma - 0.89 \delta g_1^Z$$

$$g_{Z\mathbf{p}}^h = -0.14 (\delta\kappa_\gamma - \hat{S} + Y) - 0.89 \delta g_1^Z - 1.3 W$$

EFT Validity

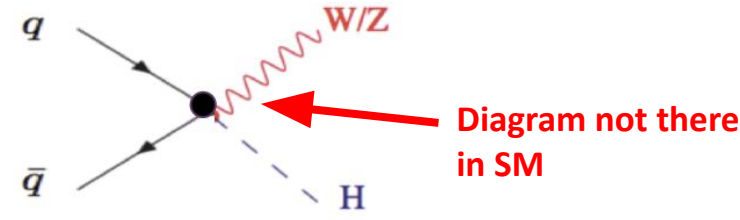
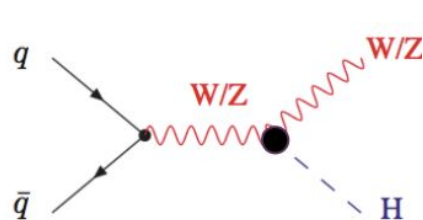
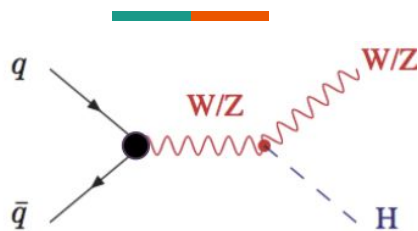
- Till now, we have dropped the $gg \rightarrow Zh$ contribution which is $\sim 15\%$ of the qq rate
- It doesn't grow with energy in presence of the anomalous couplings
- We estimate the scale of new physics for a given δg_{Zf}^h
- Example: Heavy $SU(2)_L$ triplet (singlet) vector W'^a (Z') couples to SM fermion current $\bar{f}\sigma^a\gamma_\mu f$ ($\bar{f}\gamma_\mu f$) with g_f and to the Higgs current

$iH^\dagger\sigma^a\overleftrightarrow{D}_\mu H$ ($iH^\dagger\overleftrightarrow{D}_\mu H$) with g_H

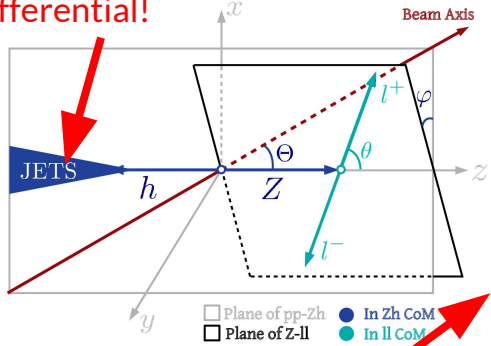
$$g_{Zf}^h \sim \frac{g_H g_f v^2}{\Lambda^2} \quad g_{Z_{u_L, d_L}}^h \sim \frac{g_H g^2 v^2}{2\Lambda^2}, \quad g_{Z_{u_R, d_R}}^h \sim \frac{g_H g' Y_{u_R, d_R} v^2}{\Lambda^2}$$

- $\Lambda \rightarrow$ mass scale of vector and thus cut-off for low energy EFT
- Assumed g_f to be a combination of $g_B = g' Y_f$ and $g_W = g/2$ for universal case

Angular observables: Zh and Wh production at the LHC (example)



Can be made more differential!



Possible to probe multiple angular observables

$$\begin{aligned}
 f_{LL} &= S_\Theta^2 S_\theta^2, \\
 f_{TT}^1 &= C_\Theta C_\theta, \\
 f_{TT}^2 &= (1 + C_\Theta^2)(1 + C_\theta^2), \\
 f_{LT}^1 &= C_\varphi S_\Theta S_\theta, \\
 f_{LT}^2 &= C_\varphi S_\Theta S_\theta C_\Theta C_\theta, \\
 \tilde{f}_{LT}^1 &= S_\varphi S_\Theta S_\theta, \\
 \tilde{f}_{LT}^2 &= S_\varphi S_\Theta S_\theta C_\Theta C_\theta, \\
 f_{TT'} &= C_{2\varphi} S_\Theta^2 S_\theta^2, \\
 \tilde{f}_{TT'} &= S_{2\varphi} S_\Theta^2 S_\theta^2,
 \end{aligned}$$

$\mathcal{O}_{H\Box} = (H^\dagger H)\Box(H^\dagger H)$	$\mathcal{O}_{HL}^{(3)} = iH^\dagger \sigma^a \overleftrightarrow{D}_\mu H \bar{L} \sigma^a \gamma^\mu L$
$\mathcal{O}_{HD} = (H^\dagger D_\mu H)^*(H^\dagger D_\mu H)$	$\mathcal{O}_{HB} = H ^2 B_{\mu\nu} B^{\mu\nu}$
$\mathcal{O}_{Hu} = iH^\dagger \overleftrightarrow{D}_\mu H \bar{u}_R \gamma^\mu u_R$	$\mathcal{O}_{HWB} = H^\dagger \sigma^a H W_{\mu\nu}^a B^{\mu\nu}$
$\mathcal{O}_{Hd} = iH^\dagger \overleftrightarrow{D}_\mu H \bar{d}_R \gamma^\mu d_R$	$\mathcal{O}_{HW} = H ^2 W_{\mu\nu} W^{\mu\nu}$
$\mathcal{O}_{He} = iH^\dagger \overleftrightarrow{D}_\mu H \bar{e}_R \gamma^\mu e_R$	$\mathcal{O}_{H\tilde{B}} = H ^2 B_{\mu\nu} \tilde{B}^{\mu\nu}$
$\mathcal{O}_{HQ}^{(1)} = iH^\dagger \overleftrightarrow{D}_\mu H \bar{Q} \gamma^\mu Q$	$\mathcal{O}_{H\tilde{W}B} = H^\dagger \sigma^a H W_{\mu\nu}^a \tilde{B}^{\mu\nu}$
$\mathcal{O}_{HQ}^{(3)} = iH^\dagger \sigma^a \overleftrightarrow{D}_\mu H \bar{Q} \sigma^a \gamma^\mu Q$	$\mathcal{O}_{H\tilde{W}} = H ^2 W_{\mu\nu}^a \tilde{W}^{a\mu\nu}$
$\mathcal{O}_{HL}^{(1)} = iH^\dagger \overleftrightarrow{D}_\mu H \bar{L} \gamma^\mu L$	$\mathcal{O}_{y_b} = y_b H ^2 (\bar{Q} H b_R + h.c.)$

CP-odd operators

Table: D6 operators in Warsaw basis contributing to anomalous $hVV^*/hV\bar{f}f$ couplings.

Mapping on to the Warsaw basis

$$\begin{aligned}
 \delta g_f^W &= \frac{g}{\sqrt{2}} \frac{v^2}{\Lambda^2} c_{HF}^{(3)} + \frac{\delta m_Z^2}{m_Z^2} \frac{\sqrt{2} g c_{\theta_W}^2}{4 s_{\theta_W}^2}, \text{ where } \frac{\delta m_Z^2}{m_Z^2} = \frac{v^2}{\Lambda^2} (2 t_{\theta_W} c_{WB} + \frac{c_{HD}}{2}) \\
 g_{Wf}^h &= \sqrt{2} g \frac{v^2}{\Lambda^2} c_{HF}^{(3)}, \quad \delta \hat{g}_{WW}^h = \frac{v^2}{\Lambda^2} \left(c_{H\Box} - \frac{c_{HD}}{4} \right) \\
 \kappa_{WW} &= \frac{2v^2}{\Lambda^2} c_{HW}, \quad \tilde{\kappa}_{WW} = \frac{2v^2}{\Lambda^2} c_{H\tilde{W}} \\
 \delta g_f^Z &= -\frac{g' Y_f}{c_{\theta_W}} c_{WB} \frac{v^2}{\Lambda^2} - \frac{g}{c_{\theta_W}} \frac{v^2}{\Lambda^2} (|T_3^f| c_{HF}^{(1)} - T_3^f c_{HF}^{(3)} + (1/2 - |T_3^f|) c_{Hf}) c_{\theta_W} \\
 &+ \frac{\delta m_Z^2}{m_Z^2} \frac{g}{2 c_{\theta_W} s_{\theta_W}^2} (T_3 c_{\theta_W}^2 + Y_f s_{\theta_W}^2) \\
 \delta \hat{g}_{ZZ}^h &= \frac{v^2}{\Lambda^2} \left(c_{H\Box} + \frac{c_{HD}}{4} \right), \quad g_{Zf}^h = -\frac{2g}{c_{\theta_W}} \frac{v^2}{\Lambda^2} (|T_3^f| c_{HF}^{(1)} - T_3^f c_{HF}^{(3)} + (1/2 - |T_3^f|) c_{Hf}) \\
 \kappa_{ZZ} &= \frac{2v^2}{\Lambda^2} (c_{\theta_W}^2 c_{HW} + s_{\theta_W}^2 c_{HB} + s_{\theta_W} c_{\theta_W} c_{HWB}) \\
 \tilde{\kappa}_{ZZ} &= \frac{2v^2}{\Lambda^2} (c_{\theta_W}^2 c_{H\tilde{W}} + s_{\theta_W}^2 c_{H\tilde{B}} + s_{\theta_W} c_{\theta_W} c_{H\tilde{W}B}) \\
 \delta \hat{g}_{bb}^h &= -\frac{v^2}{\Lambda^2} \frac{v}{\sqrt{2} m_b} c_{yb} + \frac{v^2}{\Lambda^2} \left(c_{H\Box} - \frac{c_{HD}}{4} \right)
 \end{aligned}$$

VH: Relations to the Warsaw Basis

Banerjee, Gupta, Reiness, Seth, Spannowsky, 2020

Angular observables: Zh and Wh production at the LHC (example)

- We sum over lepton polarisations and express the analogous angles (θ, φ) for the positively-charged lepton

$$\sum_{L,R} |\mathcal{A}(\hat{s}, \Theta, \theta, \varphi)|^2 = \alpha_L |\mathcal{A}_h(\hat{s}, \Theta, \theta, \varphi)|^2 + \alpha_R |\mathcal{A}_h(\hat{s}, \Theta, \pi - \theta, \pi + \varphi)|^2$$

- $\alpha_{L,R} = (g_{L,R}^Z)^2 / [(g_{L,R}^Z)^2 + (g_{R,L}^Z)^2] \rightarrow$ fraction of $Z \rightarrow \ell^+ \ell^-$ decays to leptons with left-handed (right-handed) chiralities $\epsilon_{LR} = \alpha_L - \alpha_R \approx 0.16$
- For left-handed chiralities, positive-helicity lepton \rightarrow positive-charged lepton
- For right-handed chiralities, positive-helicity lepton \rightarrow negative-charged lepton $\rightarrow (\hat{\theta}, \hat{\varphi}) \rightarrow (\pi - \theta, \pi + \varphi) \rightarrow$ Following 9 coefficients are 9 angular moments for $pp \rightarrow Z(\ell\ell)h$

$$\sum_{L,R} |\mathcal{A}(\hat{s}, \Theta, \theta, \varphi)|^2 = a_{LL} \sin^2 \Theta \sin^2 \theta + a_{TT}^1 \cos \Theta \cos \theta$$

$$+ a_{TT}^2 (1 + \cos^2 \Theta)(1 + \cos^2 \theta) + \cos \varphi \sin \Theta \sin \theta$$

$$\times (a_{LT}^1 + a_{LT}^2 \cos \theta \cos \Theta) + \sin \varphi \sin \Theta \sin \theta$$

$$\times (\tilde{a}_{LT}^1 + \tilde{a}_{LT}^2 \cos \theta \cos \Theta) + a_{TT'} \cos 2\varphi \sin^2 \Theta \sin^2 \theta$$

$$+ \tilde{a}_{TT'} \sin 2\varphi \sin^2 \Theta \sin^2 \theta$$

CP-odd
moments \rightarrow

Angular observables: Zh and Wh production at the LHC (example)

$$\epsilon_{LR} = \frac{(g_{t_R}^V)^2 - (g_{t_L}^V)^2}{(g_{t_R}^V)^2 + (g_{t_L}^V)^2}$$

$$\mathcal{G} = gg_f^Z \sqrt{(g_{t_L}^Z)^2 + (g_{t_R}^Z)^2} / (\cos \theta_W \Gamma_Z)$$

$$\gamma = \sqrt{\hat{s}} / (2m_V)$$

$$\begin{aligned} \sum_{L,R} |\mathcal{A}(\hat{s}, \Theta, \theta, \varphi)|^2 &= a_{LL} \sin^2 \Theta \sin^2 \theta + a_{TT}^1 \cos \Theta \cos \theta \\ &+ a_{TT}^2 (1 + \cos^2 \Theta)(1 + \cos^2 \theta) + \cos \varphi \sin \Theta \sin \theta \\ &\times (a_{LT}^1 + a_{LT}^2 \cos \theta \cos \Theta) + \sin \varphi \sin \Theta \sin \theta \\ &\times (\tilde{a}_{LT}^1 + \tilde{a}_{LT}^2 \cos \theta \cos \Theta) + a_{TT'} \cos 2\varphi \sin^2 \Theta \sin^2 \theta \\ &+ \tilde{a}_{TT'} \sin 2\varphi \sin^2 \Theta \sin^2 \theta \end{aligned}$$

a_{LL}	$\frac{\mathcal{G}^2}{4} [1 + 2\delta \hat{g}_{VV}^h + 4\hat{\kappa}_{VV} + 2\delta g_f^Z + \frac{g_f^h}{g_f^V} (-1 + 4\gamma^2)]$
a_{TT}^1	$\frac{\mathcal{G}^2 \sigma_{\epsilon RL}}{2\gamma^2} [1 + 4 \left(\frac{g_f^h}{g_f^V} + \hat{\kappa}_{VV} \right) \gamma^2]$
a_{TT}^2	$\frac{\mathcal{G}^2}{8\gamma^2} [1 + 4 \left(\frac{g_f^h}{g_f^V} + \hat{\kappa}_{VV} \right) \gamma^2]$
a_{LT}^1	$-\frac{\mathcal{G}^2 \sigma_{\epsilon RL}}{2\gamma} [1 + 2 \left(\frac{2g_f^h}{g_f^V} + \hat{\kappa}_{VV} \right) \gamma^2]$
a_{LT}^2	$-\frac{\mathcal{G}^2}{2\gamma} [1 + 2 \left(\frac{2g_f^h}{g_f^V} + \hat{\kappa}_{VV} \right) \gamma^2]$
\tilde{a}_{LT}^1	$-\mathcal{G}^2 \sigma_{\epsilon RL} \hat{\kappa}_{VV} \gamma$
\tilde{a}_{LT}^2	$-\mathcal{G}^2 \hat{\kappa}_{VV} \gamma$
$a_{TT'}$	$\frac{\mathcal{G}^2}{8\gamma^2} [1 + 4 \left(\frac{g_f^h}{g_f^V} + \hat{\kappa}_{VV} \right) \gamma^2]$
$\tilde{a}_{TT'}$	$\frac{\mathcal{G}^2}{2} \hat{\kappa}_{VV}$

Suppressed moments

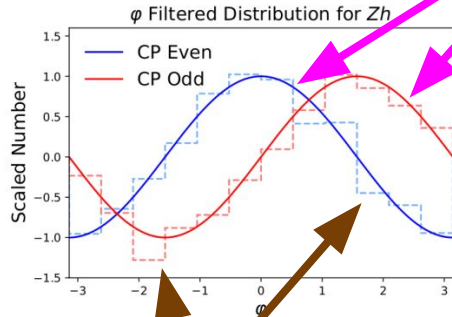
Angular observables: Zh and Wh production at the LHC (example)

Q: Are the LO theoretical shapes preserved upon the inclusion of NLO effects, radiations, showering, experimental cuts, etc.?

A: For the azimuthal angles, they are.

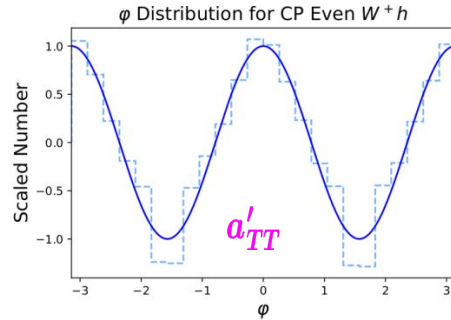
Angular moments a_{LT}^2 and \tilde{a}_{LT}^2 after weighting each event by the sign of $\sin 2\Theta \sin 2\theta$

$$\sum_{L,R} |\mathcal{A}(\hat{s}, \Theta, \theta, \varphi)|^2 = a_{LL} \sin^2 \Theta \sin^2 \theta + a_{TT}^1 \cos \Theta \cos \theta + a_{TT}^2 (1 + \cos^2 \Theta)(1 + \cos^2 \theta) + \cos \varphi \sin \Theta \sin \theta \times (a_{LT}^1 + a_{LT}^2 \cos \theta \cos \Theta) + \sin \varphi \sin \Theta \sin \theta \times (\tilde{a}_{LT}^1 + \tilde{a}_{LT}^2 \cos \theta \cos \Theta) + a_{TT'} \cos 2\varphi \sin^2 \Theta \sin^2 \theta + \tilde{a}_{TT'} \sin 2\varphi \sin^2 \Theta \sin^2 \theta$$

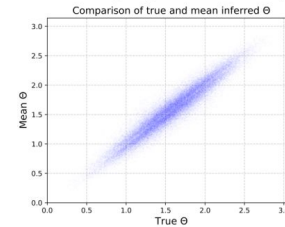


SB, Gupta, Reiness, Seth, Spannowsky, 2020

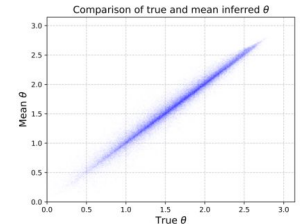
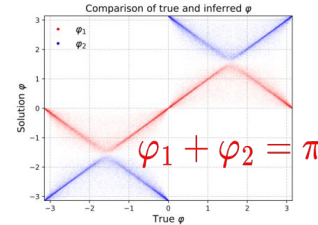
Monte Carlo samples: showering, hadronisation, passing all selection cuts



• Ambiguity in neutrino p_z



Assuming on-shell W!



Method of Moments



- An analog of **Fourier analysis** utilised to extract angular moments
- Our squared amplitude can be parametrised as,

$$|\mathcal{A}|^2 = \sum_i a_i(E) f_i(\Theta, \theta, \varphi)$$

- We look for weight functions, $w_i(\Theta, \theta, \varphi)$, such that

$$\langle w_i | f_j \rangle = \int d(\Theta, \theta, \varphi) w_i f_j = \delta_{ij}$$

- One can then pick out the angular moments, a_i as

$$a_i = \int d(\Theta, \theta, \varphi) |\mathcal{A}|^2 w_i$$

Method of Moments

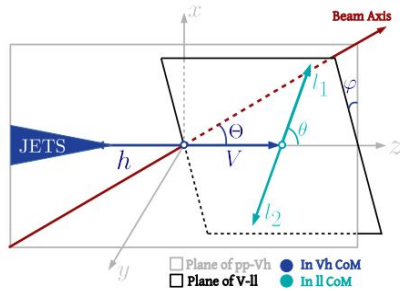
- For the set of basis functions, we get the following matrix

$$M = \begin{pmatrix} \frac{512\pi}{225} & 0 & \frac{128\pi}{25} & 0 & 0 & 0 & 0 & 0 & 0 \\ 0 & \frac{8\pi}{9} & 0 & 0 & 0 & 0 & 0 & 0 & 0 \\ \frac{128\pi}{25} & 0 & \frac{6272\pi}{225} & 0 & 0 & 0 & 0 & 0 & 0 \\ 0 & 0 & 0 & \frac{16\pi}{9} & 0 & 0 & 0 & 0 & 0 \\ 0 & 0 & 0 & 0 & \frac{16\pi}{225} & 0 & 0 & 0 & 0 \\ 0 & 0 & 0 & 0 & 0 & \frac{16\pi}{9} & 0 & 0 & 0 \\ 0 & 0 & 0 & 0 & 0 & 0 & \frac{16\pi}{225} & 0 & 0 \\ 0 & 0 & 0 & 0 & 0 & 0 & 0 & \frac{256\pi}{225} & 0 \\ 0 & 0 & 0 & 0 & 0 & 0 & 0 & 0 & \frac{256\pi}{225} \end{pmatrix}$$

- $w_i \propto f_i$ except for $i = 1, 3$
- We rotate the (1,3) system to an orthogonal basis
- Using discrete method, we find: $a_i(M) = \frac{\hat{N}}{N} \sum_{n=1}^N w_i(\Theta_n, \theta_n, \varphi_n)$
- Events divided in bins of final state invariant mass ($M \rightarrow$ central value of bin), $N(M)(N(\hat{M})) \rightarrow$ number of MC (actual) events in that bin for a fixed integrated luminosity

Angular observables: $Vh \rightarrow 2lbb$ and $ggF (h \rightarrow ZZ^* \rightarrow 4l)$

$$Vh \left(\frac{d\sigma}{dE d\Theta d\theta d\varphi} \right)$$



$$f_{LL} = S_{\Theta}^2 S_{\theta}^2,$$

$$f_{TT}^1 = C_{\Theta} C_{\theta},$$

$$f_{TT}^2 = (1 + C_{\Theta}^2)(1 + C_{\theta}^2),$$

$$f_{LT}^1 = C_{\varphi} S_{\Theta} S_{\theta},$$

$$f_{LT}^2 = C_{\varphi} S_{\Theta} S_{\theta} C_{\Theta} C_{\theta},$$

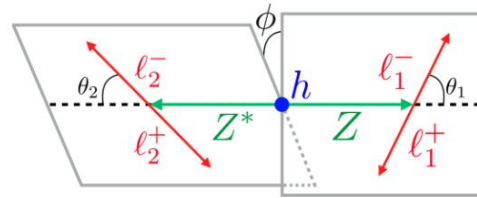
$$\tilde{f}_{LT}^1 = S_{\varphi} S_{\Theta} S_{\theta},$$

$$\tilde{f}_{LT}^2 = S_{\varphi} S_{\Theta} S_{\theta} C_{\Theta} C_{\theta},$$

$$f_{TT'} = C_{2\varphi} S_{\Theta}^2 S_{\theta}^2,$$

$$\tilde{f}_{TT'} = S_{2\varphi} S_{\Theta}^2 S_{\theta}^2,$$

$$ggF \left(\frac{d\sigma}{dE d\theta_1 d\theta_2 d\phi} \right)$$



$$f_1 = \sin^2(\theta_1) \sin^2(\theta_2)$$

$$f_2 = (\cos^2(\theta_1) + 1)(\cos^2(\theta_2) + 1)$$

$$f_3 = \sin(2\theta_1) \sin(2\theta_2) \cos(\phi)$$

$$f_4 = (\cos^2(\theta_1) - 1)(\cos^2(\theta_2) - 1) \cos(2\phi)$$

$$f_5 = \sin(\theta_1) \sin(\theta_2) \cos(\phi)$$

$$f_6 = \cos(\theta_1) \cos(\theta_2)$$

$$f_7 = (\cos^2(\theta_1) - 1)(\cos^2(\theta_2) - 1) \sin(2\phi)$$

$$f_8 = \sin(\theta_1) \sin(\theta_2) \sin(\phi)$$

$$f_9 = \sin(2\theta_1) \sin(2\theta_2) \sin(\phi),$$

SB, Englert, Gupta, Spannowsky, 2018

SB, Gupta, Ochoa-Valeriano, Spannowsky, Venturini, 2020

Angular observables: Gluon fusion in golden channel (example)

- Angular differential distributions, modified in the EFT

$$\begin{aligned}
 a_1 &= \mathcal{G}^4 \left((1 + \delta a) + \frac{bm_{Z^*}\gamma_b^2}{m_Z\gamma_a} \right)^2 \\
 a_2 &= \mathcal{G}^4 \left(\frac{(1 + \delta a)^2}{2\gamma_a^2} + \frac{2c^2m_{Z^*}^2\gamma_b^2}{m_Z^2\gamma_a^2} \right) \\
 a_3 &= -\mathcal{G}^4 \left(\frac{1 + \delta a}{2\gamma_a} + \frac{bm_{Z^*}\gamma_b^2}{2m_Z\gamma_a} \right)^2 \\
 a_4 &= \mathcal{G}^4 \left(\frac{(1 + \delta a)^2}{2\gamma_a^2} - \frac{2c^2m_{Z^*}^2\gamma_b^2}{m_Z^2\gamma_a^2} \right) \\
 a_5 &= -\epsilon^2\mathcal{G}^4 \left(\frac{2(1 + \delta a)^2}{\gamma_a} + \frac{2(1 + \delta a)bm_{Z^*}\gamma_b^2}{m_Z\gamma_a^2} \right) \\
 a_6 &= \epsilon^2\mathcal{G}^4 \left(\frac{2(1 + \delta a)^2}{\gamma_a^2} + \frac{8c^2m_{Z^*}^2\gamma_b^2}{m_Z^2\gamma_a^2} \right) \\
 a_7 &= \mathcal{G}^4 \frac{2(1 + \delta a)cm_{Z^*}\gamma_b}{m_Z\gamma_a^2} \\
 a_8 &= -\epsilon^2\mathcal{G}^4 \left(\frac{4(1 + \delta a)cm_{Z^*}\gamma_b}{m_Z\gamma_a} + \frac{4bcm_{Z^*}^2\gamma_b^3}{m_Z^2\gamma_a^2} \right) \\
 a_9 &= \mathcal{G}^4 \left(\frac{(1 + \delta a)cm_{Z^*}\gamma_b}{m_Z\gamma_a} + \frac{bcm_{Z^*}^2\gamma_b^3}{m_Z^2\gamma_a^2} \right),
 \end{aligned}$$

1 → SM

$$\delta a = \delta g_{ZZ}^h - \kappa_{ZZ}\gamma_a \frac{m_{Z^*}}{m_Z} \frac{m_Z^2 - m_{Z^*}^2}{2m_Z^2}$$

$$b = \kappa_{ZZ}$$

$$c = -\frac{\tilde{\kappa}_{ZZ}}{2}$$

$$\begin{aligned}
 \mathcal{G}^4 &= ((g_L^Z)^2 + (g_R^Z)^2)((g_L^{Z^*})^2 + (g_R^{Z^*})^2) \\
 \epsilon^2\mathcal{G}^4 &= ((g_L^Z)^2 - (g_R^Z)^2)((g_L^{Z^*})^2 - (g_R^{Z^*})^2),
 \end{aligned}$$

Small → a_5, a_6 and a_8 suppressed

a_7, a_8, a_9 CP-odd

SB, Gupta,
Ochoa-Valeriano,
Spannowsky, Venturini,
2020

[Slide courtesy Elena Venturini]

Theory uncertainties in EFT analyses



1. Ambiguities in operator coefficients  **uncertainties in coefficients of remaining operators**
2. Validity of perturbative expansion (Rick might cover this, time permitting)
3. Renormalisation Group Evolution (RGE) effects alter behaviour of theory under RGE  describes **how EFT couplings vary with energy scales**  **uncertainties in predicted energy dependence of observables (If time permitting)**
4. Can lead to **inconsistencies while matching to a model**

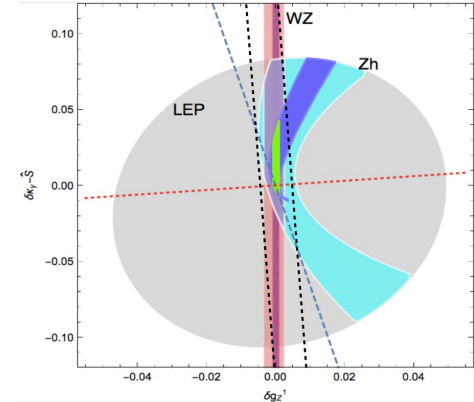
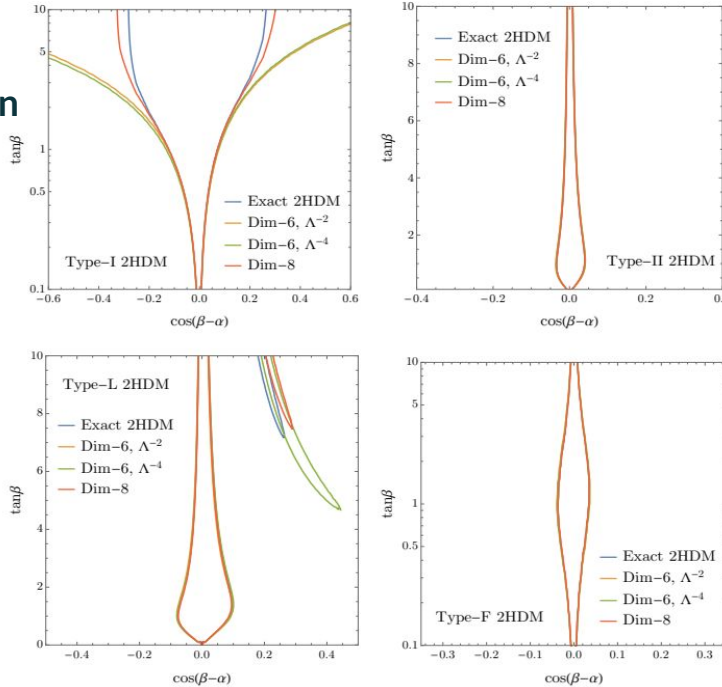
Theory uncertainties in EFT analyses: operator truncation



Example showing the importance of truncation of operators to match specific models for a top-down approach!

Dawson et al, 2022

See Joydeep's presentation for a detailed look on top-down versus bottom-up approaches!



In parameter space of interest linear term dominates the squared term!

SB, Englert, Gupta, Spannowsky, 2018

Theory uncertainties in EFT analyses: TGCs



1. EFT operators contributing to anomalous charged triple gauge couplings (cTGCs) and anomalous neutral triple gauge couplings (nTGCs)  treated separately!
2. For cTGCs, D8 operators are usually not considered
3. For nTGCs, D8 operators are usually the first ones to show effects. Some such operators also contribute to cTGCs
4. **Necessary to consider TGCs through a holistic approach!**

Theory uncertainties in EFT analyses: TGCs

1. Relevant operators for TGCs at dimension-6 (D6) X^3 ($X = W, B$ field strength tensor)
2. Relevant operators for TGCs at dimension-8 (D8)
 $X^2\phi^2D^2, X^2\psi^2D$ ($\phi =$ Higgs field, $\psi =$ fermion fields, $D =$ covariant derivative)
3. These classes of operators contribute to TGCs and it is crucial to consider them in conjunction

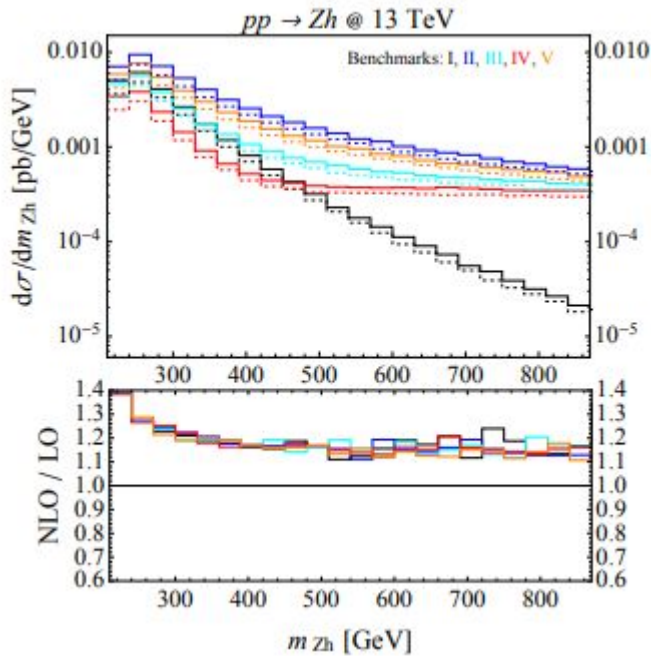
$$\begin{aligned} \dot{C}_G &= (12c_{A,3} - 3b_{0,3}) g_3^2 C_G & \dot{C}_{\tilde{G}} &= (12c_{A,3} - 3b_{0,3}) g_3^2 C_{\tilde{G}} \\ \dot{C}_W &= (12c_{A,2} - 3b_{0,2}) g_2^2 C_W & \dot{C}_{\tilde{W}} &= (12c_{A,2} - 3b_{0,2}) g_2^2 C_{\tilde{W}} \end{aligned}$$

	$\phi^4 D^4$		$\psi^2 B \phi^3$	$\psi^2 W \phi^3$	$\psi^2 G \phi^3$	$\psi^2 \phi^2 D^3$
$B^2 \phi^2 D^2$	g_1^2	$B^2 \phi^2 D^2$	0	0	0	g_1^2
$W^2 \phi^2 D^2$	g_2^2	$W^2 \phi^2 D^2$	0	0	0	g_2^2
$WB \phi^2 D^2$	$g_1 g_2$	$WB \phi^2 D^2$	0	0	0	$g_1 g_2$

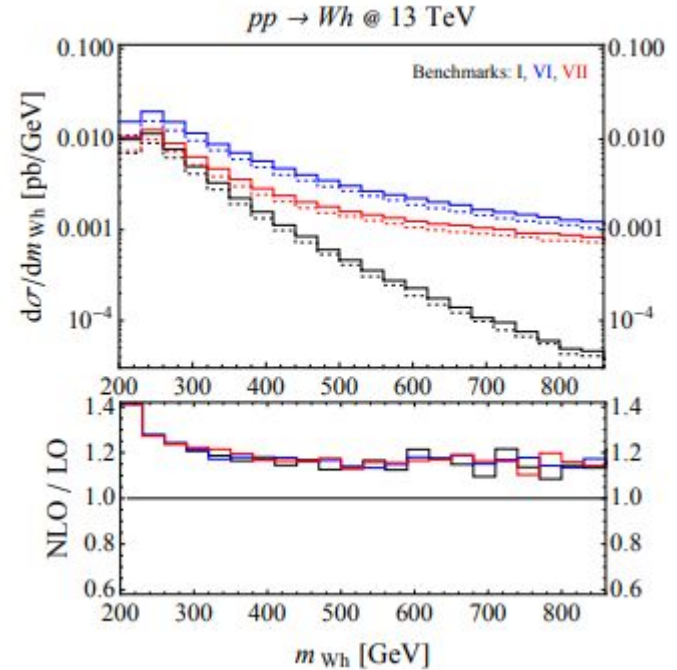
[Alonso et al, 2013](#)

[Das Bakshi et al, 2022](#)

Theory uncertainties in EFT analyses: NLO effects (QCD)



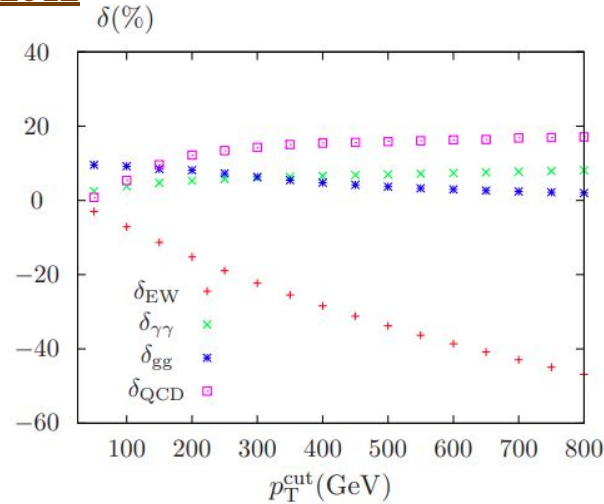
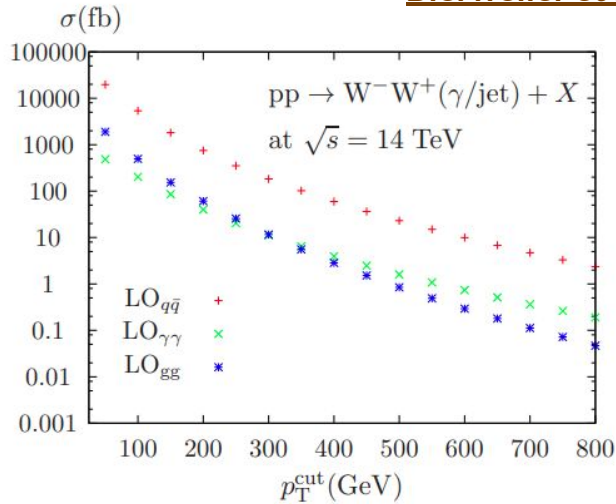
Automated in
MG5_aMC@N
LO through
NLOCT!



Greljo et al, 2017

Theory uncertainties in EFT analyses: NLO effects (EW)

Bierweiler et al, 2012



Corrections to $W+W-$ production for 14 TeV LHC in SM.

Electroweak corrections are quite large!

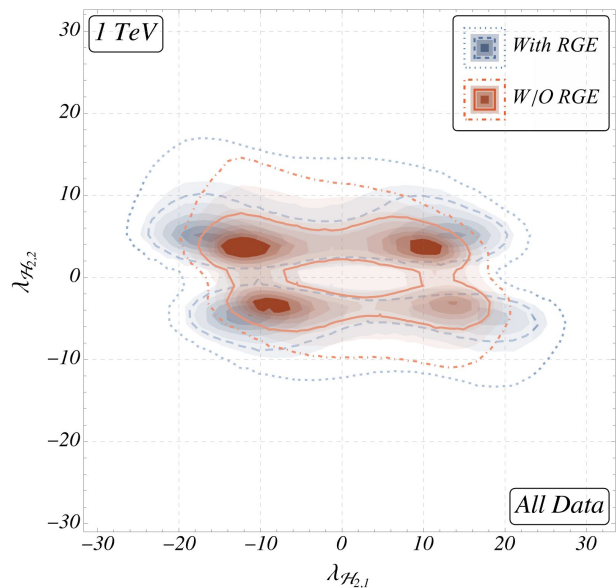
In the era of precision physics when SM backgrounds will be considered at NNLO QCD + NLO EW, the BSM signal sample needs to compete!

At energies surpassing the electroweak scale, quasi-massless electroweak bosons lead to $\delta_{EW} = \mathcal{O}(-10\%)$ corrections.

$\delta_{EW} = \frac{\sigma_{NLO}^{EW}}{\sigma_{LO}}$ For large transverse momenta, the EW and QCD corrections are comparable!

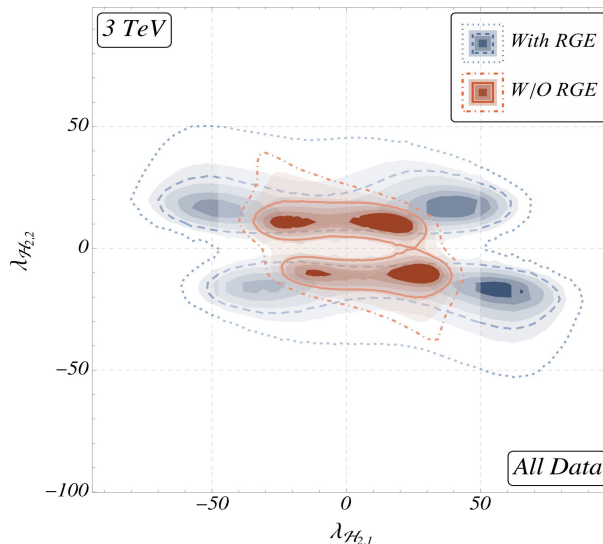
Forthcoming work with Reichelt and Spannowsky

Theory uncertainties in EFT analyses: RGE effects



Usually, the running of the SMEFT operators ignored which emerge at Λ . But, observables at EW scale

For 2HDM, 51 operators generated of which 14 are from RGE!



Increase in mass scale relaxes the parameter bounds!

Anisha et al, 2021

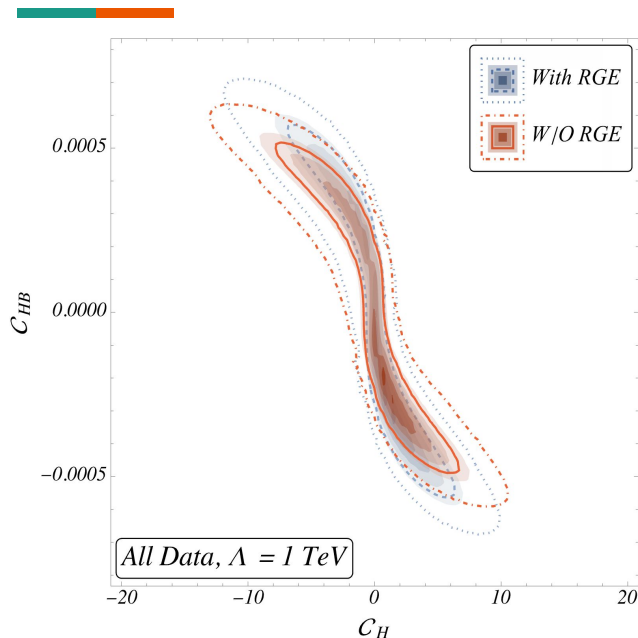
At LO

Parameter space relaxed after considering RGE!

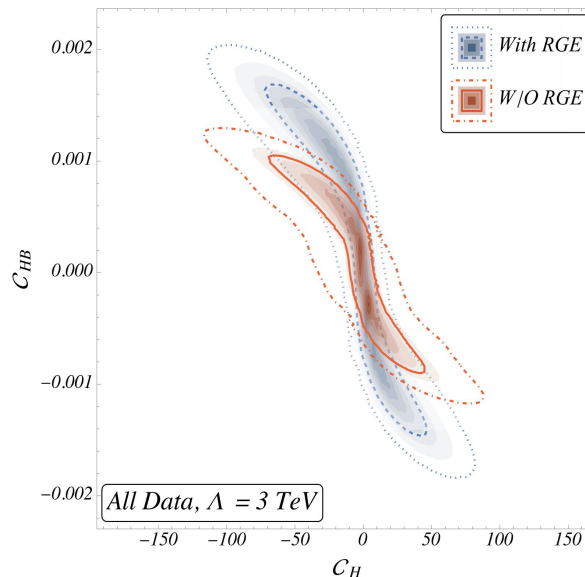
$$C_i(M_Z) = C_i(\Lambda) + \sum_j \frac{1}{16\pi^2} \gamma_{ij} C_j(\Lambda) \log\left[\frac{M_Z}{\Lambda}\right]$$

$$\frac{dC_i(\mu)}{d\log(\mu)} = \sum_j \frac{1}{16\pi^2} \gamma_{ij} C_j \quad \text{Leading log approximation}$$

Theory uncertainties in EFT analyses: RGE effects



Usually, the running of the SMEFT operators ignored which emerge at Λ .
But, observables at EW scale



For 2HDM, 51 operators generated of which 14 are from RGE!

Anisha et al, 2021

At LO

$$C_i(M_Z) = C_i(\Lambda) + \sum_j \frac{1}{16\pi^2} \gamma_{ij} C_j(\Lambda) \log\left[\frac{M_Z}{\Lambda}\right]$$

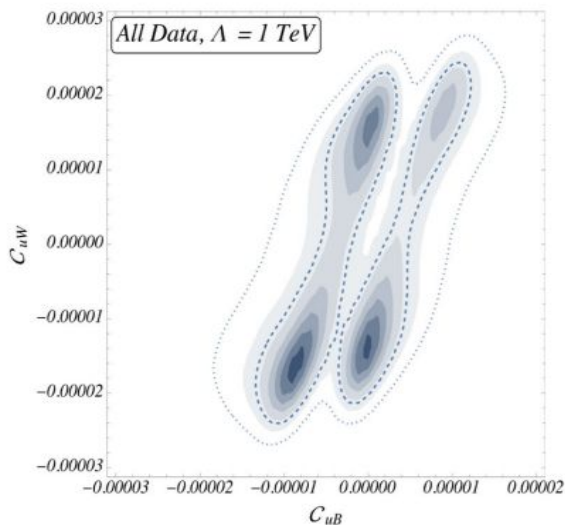
$$\frac{dC_i(\mu)}{d\log(\mu)} = \sum_j \frac{1}{16\pi^2} \gamma_{ij} C_j$$

Theory uncertainties in EFT analyses: RGE effects

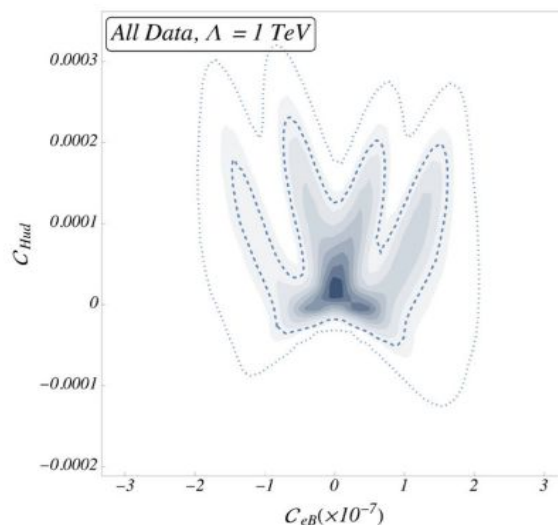
Usually, the running of the SMEFT operators ignored which emerge at Λ .
But, observables at EW scale

For 2HDM, 51 operators generated (top-down matching) of which 14 are from RGE! Examples (all suppressed by $16\pi^2$):

$\mathcal{O}_{uB}, \mathcal{O}_{uW}, \mathcal{O}_{dB}, \mathcal{O}_{dW}, \mathcal{O}_{eB}, \mathcal{O}_{eW}, \mathcal{O}_{Hud}$



(a) $C_{uB} - C_{uW}$



(b) $C_{eB} - C_{Hud}$

Anisha et al.
2021

Electroweak corrections



We include approximate electroweak (EW) corrections in Sherpa which includes infrared subtracted EW 1-loop corrections as additional weights to the respective Born cross sections. In those the event weight is calculated based on the expression

$$d\sigma_{\text{NLO,EW}_{\text{approx}}} = [B(\Phi) + V_{\text{EW}}(\Phi) + I_{\text{EW}}(\Phi)] d\Phi$$

B = Born contribution also entering the uncorrected QCD cross Section

V_{EW} = electroweak virtual corrections at 1-loop accuracy

I_{EW} = generalised Catani-Seymour insertion operator for EW NLO calculations.

Latter subtracts all infrared singularities of the virtual corrections. This fundamentally arbitrary procedure should provide a good approximation if electroweak Sudakov logarithms are dominant.



Catani-Seymour

The Catani-Seymour subtraction method, including the use of the insertion operator $\mathbf{I}(\epsilon)$, was originally developed for handling infrared (IR) divergences in Quantum Chromodynamics (QCD) calculations. However, the principles behind the subtraction method can be extended and applied to other gauge theories, including electroweak (EW) theory, for next-to-leading-order (NLO) calculations.

Application to Electroweak Calculations

When dealing with NLO corrections in electroweak (EW) theory, similar challenges arise due to IR divergences from soft and collinear photons (and sometimes Z bosons in specific processes). The Catani-Seymour subtraction method can be adapted to manage these divergences as follows:

1. **Photon Emission**: Just as gluons can be soft or collinear in QCD, photons can be emitted in a soft or collinear manner, leading to IR divergences. The subtraction terms in the Catani-Seymour method can be modified to account for the specific kinematics and coupling structures of photon emissions.



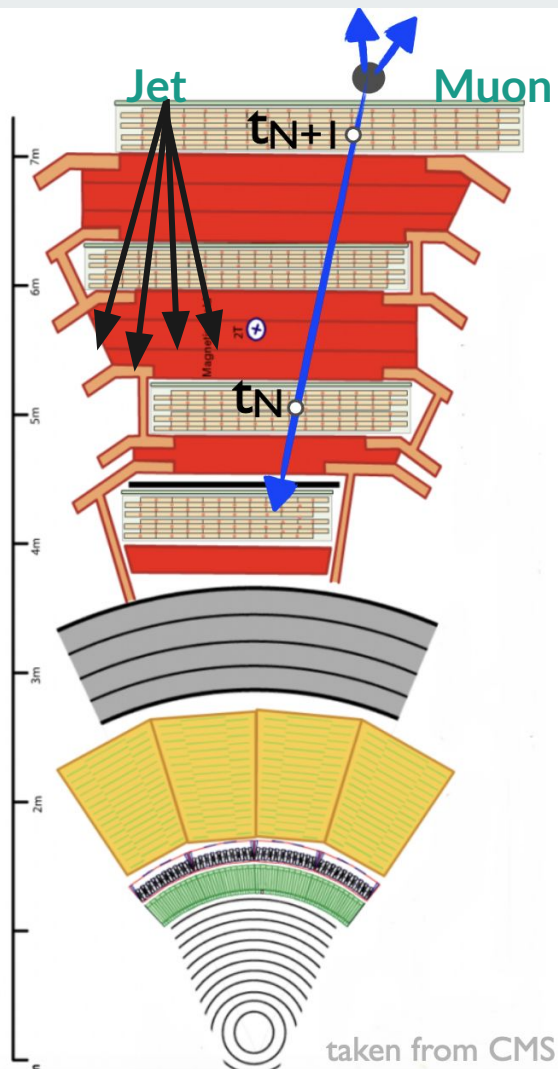
Catani Seymour

2. **Universal Structures**: The structure of IR divergences has universal properties that apply across different gauge theories. The key idea of constructing counterterms that locally approximate the behavior of the matrix elements in singular regions remains valid.

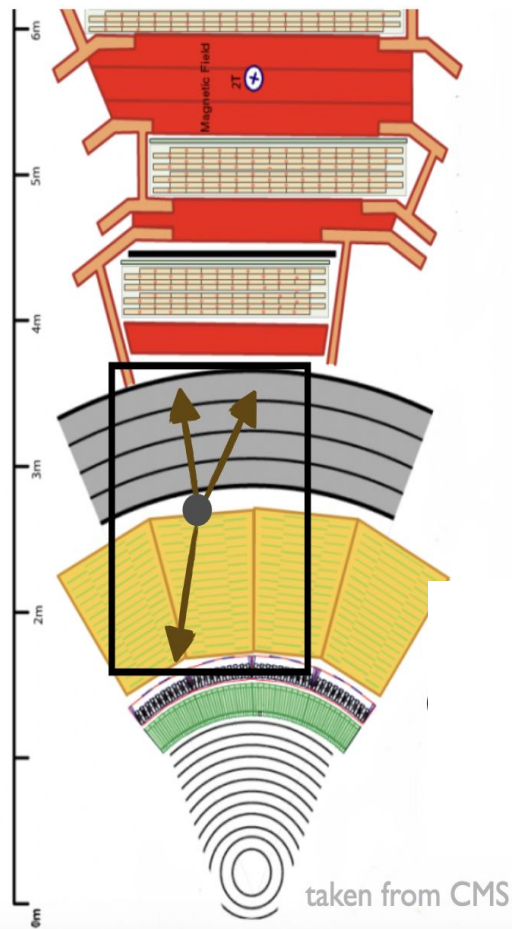
3. **Insertion Operators**: In the EW context, the insertion operator $\mathbf{I}(\epsilon)$ must be redefined to include the contributions from the EW interactions. This involves recalculating the kinematic factors $\mathcal{V}_{ij}(\epsilon)$ to reflect the dynamics of photons (and possibly other weak bosons).

4. **Mixed QCD-EW Corrections**: In processes involving both QCD and EW corrections, a combined subtraction scheme can be employed. This involves constructing subtraction terms that handle both QCD and EW singularities simultaneously, ensuring a consistent treatment of all IR divergences.

Decay outside the detector



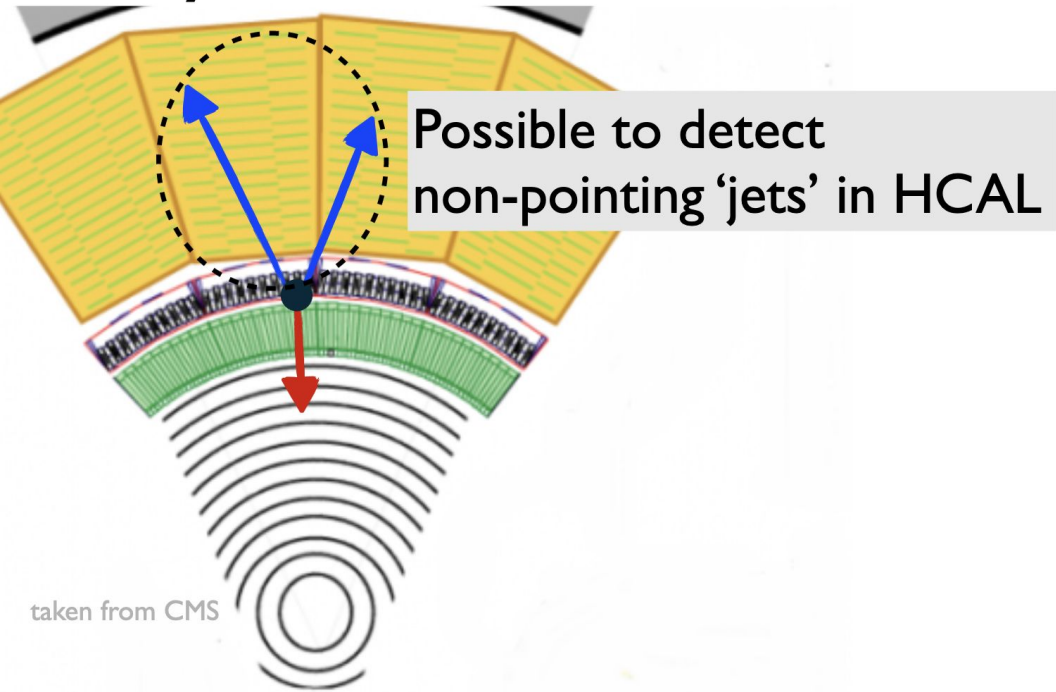
- If muons are the Backward moving objects (BMOs):
 - In such a scenario, we gain by using backward moving objects (BMOs) since they are the only ones that can be detected
 - Huge background from cosmic muons
 - Can focus on the lower half of the barrel?
 - Since cosmic muon traverses the full detector, we will have mip timing layer with a timing precision of 20 ps. So we can require
 - $\text{Time}_{\text{mip_lower}} < \text{Time}_{\text{mip_upper}}$ since the BMO is traveling from lower half to the upper half
 - In addition, we can require the timing difference between different RPC layers to tag muons traveling from lower half towards the center of the CMS detector (timing resolution of RPCs ~ 3 ns)
- If hadrons are the BMOs:
 - It looks like an inverted shower in the muon chambers \rightarrow easy to tag?



Decay outside HCAL

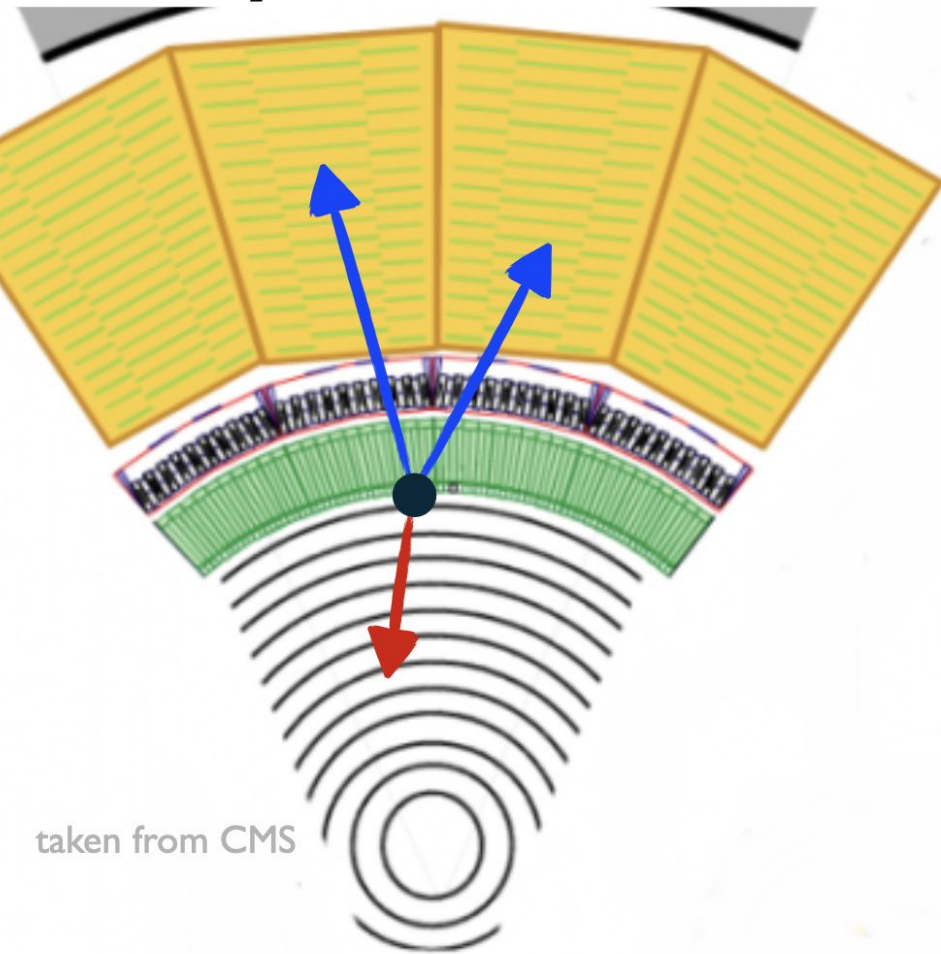
- Again inverted jets like before
- Require the Energy in outer layer $<$ Energy in the inner layer?

Additional handles to decay outside ECAL



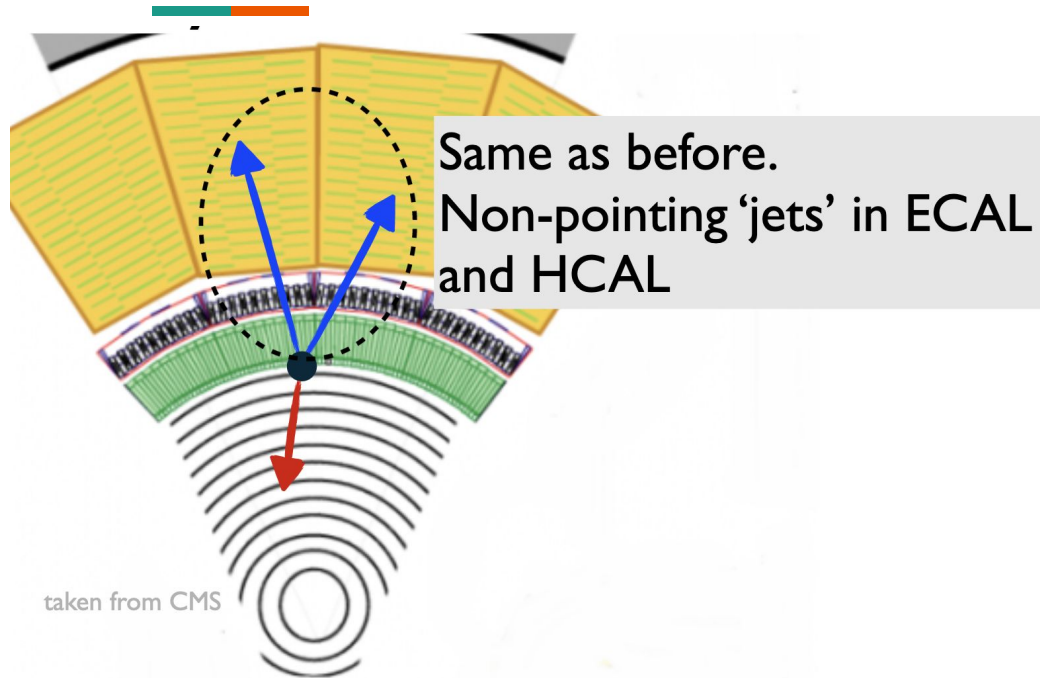
taken from CMS

Decays outside the tracker

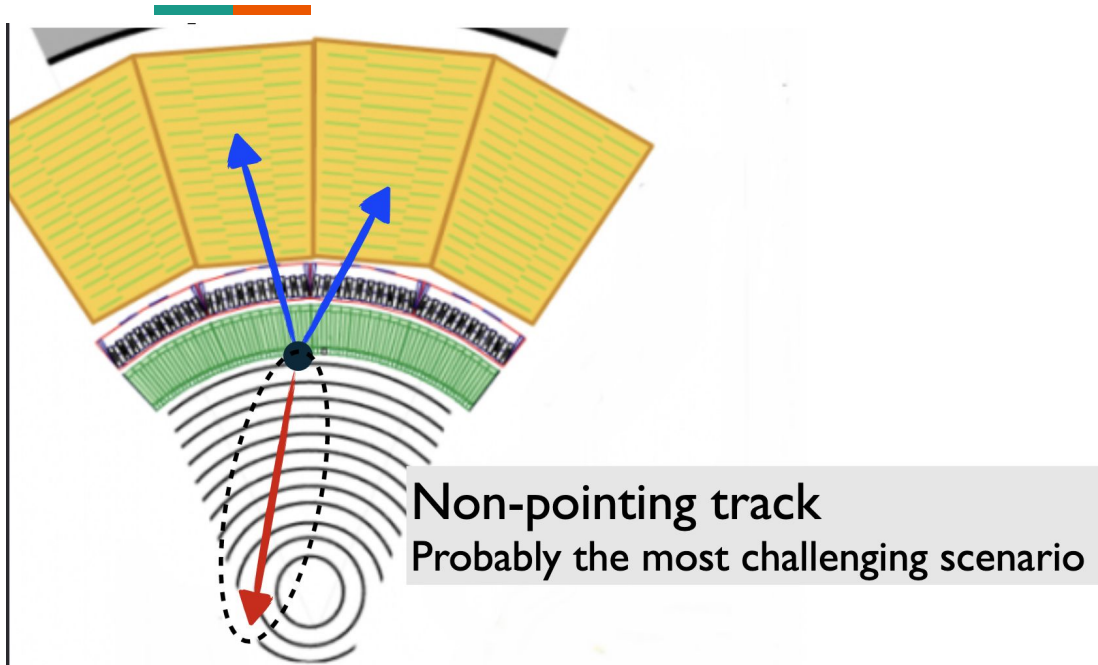


taken from CMS

Decays outside the tracker



Decays outside the tracker



taken from CMS

- Large impact parameter of such non-pointing tracks
 - In case of quark that hadronised → expect to see cluster of tracks originating from a common point with large impact parameter
- After normal tracking is done, use the left hits for inward moving tracks?